CONFIDENTIAL

Copy
RM H54H16

NACA RM H54H16

NACA

RESEARCH MEMORANDUM

LONGITUDINAL STABILITY CHARACTERISTICS IN ACCELERATED MANEUVERS AT SUBSONIC AND TRANSONIC SPEEDS OF THE DOUGLAS D-558-II RESEARCH AIRPLANE EQUIPPED WITH A LEADING-EDGE WING CHORD-EXTENSION

By Jack Fischel and Cyril D. Brunn

High-Speed Flight Station
Edwards, Calif.

NATIONAL ADVISORY COMMITTEE
FOR AERONAUTICS

WASHINGTON

October 27, 1954

CONFIDENTIAL

NATIONAL ADVISORY COMMITTEE FOR AERONAUTICS

RESEARCH MEMORANDUM

LONGITUDINAL STABILITY CHARACTERISTICS IN ACCELERATED MANEUVERS AT SUBSONIC AND TRANSONIC SPEEDS OF THE DOUGLAS D-558-II RESEARCH AIRPLANE EQUIPPED WITH A LEADING-EDGE WING CHORD-EXTENSION

By Jack Fischel and Cyril D. Brunn

SUMMARY

Previous flight tests of the Douglas D-558-II research airplane revealed a reduction in longitudinal stability and pitch-up which is characteristic of current swept-wing airplanes. Various wind-tunnel investigations, including investigations on a model of the subject airplane, indicated that wing leading-edge chord-extensions would tend to alleviate the unstable longitudinal characteristics of swept-wing airplanes; therefore, the airplane was modified to include wing-chord extensions, and was flight tested. The chord-extensions were of constant chord and extended from the 68-percent semispan station to the wing tip. No wing fences were installed for these tests, which were performed in the clean condition in the altitude range from 18,800 feet to 34,000 feet and at Mach numbers from about 0.45 to 1.0.

Addition of wing-chord extensions had only a minor effect on the initial decay in stick-fixed stability (pitch-up) and stick-free stability experienced by the airplane at moderate angles of attack. The chord-extensions alleviated the pitch-up to a small degree, but the pilot still considered the airplane unsatisfactory for controlled accelerated flight in this region. However, at the higher angles of attack, the airplane appeared to retrim and regain some stability. The normal-force coefficient at which the decay in stick-fixed stability occurred decreased from a value of about 0.75 at a Mach number of 0.5 to about 0.46 at a Mach number of 0.88, and then increased to about 0.55 at a Mach number of 0.93. A value of normal-force coefficient of 0.76 was attained at a Mach number of 0.98 with no apparent reduction in stability.

The buffeting of the airplane was of such a nature that the increase in buffet intensity induced by the chord-extensions became a major problem, in addition to the longitudinal-instability problem.

A comparison of wind-tunnel data with flight data showed good agreement in the reduction of stability evident at moderate angles of attack. The results indicated that an abrupt reduction of stability to a region of neutral or even slight stability could tend to cause pitch-up. Subsequent to the performance of the subject flight investigation, an analytical method (RM L53I02) was formulated to calculate airplane response to longitudinal control input, using wind-tunnel data. Comparison of results obtained by this method appeared to give fairly accurate correlation with flight results.

At low lift coefficients the trends in the values of the slope of the airplane normal-force-coefficient curve $dC_{N_A}/d\alpha$, the apparent stability parameter $d\delta_e/dC_{N_A}$, and the elevator control force parameter dF_e/dn were little affected by the addition of wing chord-extensions. However, addition of the wing chord-extensions caused the airplane stick-fixed neutral point to move forward about 3 percent mean aerodynamic chord.

INTRODUCTION

Associated with the use of sweptback wings on aircraft is the occurrence of a reduction of longitudinal stability at moderate lift coefficients which is attributable, directly or indirectly, to the effects of wing-tip separation. This reduction of stability results, in some instances, in an uncontrolled pitching of the airplane to large angles of attack (refs. 1 to 5). As a result, the normal-force coefficient—Mach number range for controlled maneuvering of the swept-wing airplane is limited, and the danger of exceeding airplane structural limits is greatly increased.

The National Advisory Committee for Aeronautics is investigating in flight the Douglas D-558-II swept-wing research airplane with various modifications designed to alleviate swept-wing instability and pitch-up. The effects of various wing fence and wing slat modifications on the airplane longitudinal stability characteristics were previously reported in references 2 and 5, and were shown to have little effect on the normal-force coefficient—Mach number boundary for unsatisfactory maneuvering stability. However, the fully extended wing slats were shown to provide somewhat improved stability characteristics at large angles of attack except in the Mach number region between about 0.80 and 0.95 (ref. 5).

Wind-tunnel studies (refs. 6, 7, and unpublished data) of the D-558-II airplane at low and high subsonic speeds indicated that the appreciable unstable break in the pitching-moment curves at moderate angles of attack, characteristic of the basic airplane configuration, was generally altered to a region of neutral or slightly positive stability with the addition of wing leading-edge chord-extensions. However, these wind-tunnel studies showed that a decrease in static stability was still apparent at moderate angles of attack with the wing chord-extensions. The evaluation of such static wind-tunnel results in terms of maneuvering handling qualities can be exceedingly difficult considering the possible importance of such dynamic effects as control-system characteristics, piloting technique (including rate of control input), buffeting, and other effects, although some progress has been made recently along these lines. (See ref. 8.) It was therefore considered desirable to perform a flight evaluation of the effects of wing chord-extensions similar to those developed in the aforementioned wind-tunnel studies to determine the effects of the discussed changes in the pitching-moment curves. Data obtained during accelerated longitudinal maneuvers up to high values of normal-force coefficient and at speeds up to a Mach number of approximately 1.0 are presented herein. Also included are some comparisons of flight with wind-tunnel data and the effects of the chord-extensions on the stability and control characteristics.

SYMBOLS

b	wing span, ft
C_m	pitching-moment coefficient
C_{N_A}	airplane normal-force coefficient
$\bar{c}$	wing mean aerodynamic chord (M.A.C.), ft
F_e	elevator control force, lb
g	acceleration due to gravity, ft/sec^2
h_p	pressure altitude, ft
i_t	stabilizer setting with respect to fuselage center line, positive when leading edge of stabilizer is up, deg
M	free-stream Mach number
n	normal acceleration, g units

t	time, sec
α	angle of attack of airplane center line, deg
δ_e	elevator deflection with respect to stabilizer, deg
$\delta_{e(\ddot{\theta} = 0)}$	elevator deflection corrected to zero pitching acceleration, deg
$\dot{\theta}$	pitching velocity, radians/sec
$\ddot{\theta}$	pitching acceleration, radians/sec^2
$dC_m/d\delta_e$	rate of change of pitching-moment coefficient with elevator deflection (elevator pitching-effectiveness parameter), per deg
$dC_{N_A}/d\alpha$	rate of change of airplane normal-force coefficient with angle of attack, per deg
$d\delta_e/dC_{N_A}$	rate of change of elevator deflection with airplane normal-force coefficient, deg
dF_e/dn	rate of change of elevator control force with normal acceleration, lb/g

AIRPLANE

The Douglas D-558-II airplanes have sweptback wing and tail surfaces and were designed for combination turbojet and rocket power. The airplane used in the present investigation (BuAero No. 37975 or NACA 145) is equipped with a Westinghouse J-34-WE-40 turbojet engine, which exhausts out the bottom of the fuselage between the wing and the tail, and with a Reaction Motors, Inc. LR8-RM-6 rocket engine, which exhausts out the rear of the fuselage. The airplane is equipped with an adjustable stabilizer. No aerodynamic balance or control-force booster system is used on the elevator. Hydraulic dampers are installed on all the control surfaces to aid in the prevention of control-surface "buzz." The airplane is air-launched from a Boeing B-29 mother airplane.

Photographs of the airplane fitted with chord-extensions are shown in figure 1, and a three-view drawing of the modified airplane is shown as figure 2. Pertinent airplane dimensions and characteristics of the unmodified airplane are listed in table I. Addition of the wing-chord-extensions increased the wing area to 181.2 square feet and the wing mean aerodynamic chord to 90.0 inches; however, for convenience in

comparison of the data herein with data for the unmodified airplane, all data presented are based on the dimensions of the unmodified airplane.

The constant chord 9.25-inch ($0.106\bar{c}$) chord-extensions added to the outer 0.32 semispan of each wing panel were similar in plan form and chord to those tested on a model of the D-558-II airplane and found to provide an improvement in static longitudinal stability at moderate angles of attack (refs. 6, 7, and unpublished data). The profiles of the chord-extensions were approximately the NACA 63-008 airfoil profile in the streamwise direction and were faired into the wing profile over the span of the chord-extensions. In addition, the chord-extensions were faired into the wing tips, and the inboard ends were flat-sided in the vertical streamwise plane (figs. 1 and 3). The wing slats, which spanned the unmodified wing panels from $0.434b/2$ to the wing tips, were cut at the $0.68b/2$ wing station and the inboard section of each slat was firmly attached to the wing in the closed position to maintain the original wing profile and plan form inboard of the $0.68b/2$ station. There were no wing fences installed during the tests of the chord-extensions.

INSTRUMENTATION

Among the standard NACA recording instruments installed in the airplane to obtain flight data were instruments which measured the following quantities pertinent to this investigation:

Airspeed
Altitude
Elevator wheel force
Normal acceleration
Pitching velocity
Pitching acceleration
Angle of attack
Stabilizer and elevator positions

All of the instruments were synchronized by means of a common timer.

The elevator position was measured at the inboard end of the control surface, and the stabilizer position was measured at the plane of symmetry. All control positions were measured perpendicular to the control hinge line.

An NACA high-speed pitot-static tube (type A-6 of ref. 9) was mounted on a boom $4\frac{3}{4}$ feet forward of the nose of the airplane. The vane used to measure the angle of attack was mounted on the same boom about $3\frac{1}{2}$ feet

forward of the nose of the airplane. The angle-of-attack data have not been corrected for the effects of upwash ahead of the nose of the airplane nor for the effects of airplane pitching velocity. However, such corrections are believed to be small and to have a negligible effect on the analysis of the data. The airspeed system was calibrated up to $M = 0.80$ by the "fly-by" method and at speeds in excess of $M = 0.80$ by the NACA radar phototheodolite method (ref. 10). The possible Mach number errors are about ± 0.01 at $M < 0.8$ and about ± 0.02 at $M \approx 0.95$.

TESTS, RESULTS, AND DISCUSSION

The longitudinal stability characteristics of the D-558-II airplane equipped with wing leading-edge chord-extensions were determined in turning flight, with flaps and landing gear up, for a range of Mach numbers from about 0.45 to about 1.0. Data were obtained in the altitude range from 18,800 feet to 34,000 feet and for two conditions of airplane center-of-gravity location, ranging from 22.6 to 24.7 and from 28.0 to 28.2 percent of the wing mean aerodynamic chord. Only a few maneuvers were performed at the rearward center-of-gravity location, inasmuch as these results (and the wind-tunnel results of refs. 6, 7, and unpublished data) indicated that the airplane had less static stability for a given center-of-gravity location when chord-extensions were installed. All remaining maneuvers with the chord-extensions were subsequently performed at the forward center-of-gravity location, which was selected to provide about the same static stability as existed with the unmodified airplane having its center of gravity at about 26 to 27 percent mean aerodynamic chord.

In general, two techniques were employed by the pilot to investigate the longitudinal handling qualities of the airplane through a lift range at various Mach numbers. In wind-up turns performed during the first flight with the chord-extension configuration, the pilot usually applied increasing up-elevator deflection until a decay in stick-fixed stability or a pitch-up was detected at which point the controls were reversed to effect a recovery from the maneuver. In this type maneuver neither the pitching velocity nor pitching acceleration was permitted to build up to appreciable values. In maneuvers performed during subsequent flights, the pilot applied increasing up-elevator deflection after detecting the region of unsatisfactory stability, in order to determine the characteristics of the airplane in this region and at the higher regions of lift and angle of attack, and then effected a recovery from the maneuver. In maneuvers of this type large values of pitching velocity and pitching acceleration were sometimes encountered, especially at the higher speeds, as is shown in the data plots. At $M > 0.9$, the aforementioned technique was modified because both elevator and stabilizer were required to perform the turns.

Data obtained in several of the turns are plotted in the form of time histories in figure 4 and as functions of angle of attack, normal-force coefficient, and normal acceleration in figure 5. It will be noted that in several instances, complete data are not presented for each maneuver because of instrumentation malfunctions during flight. Additional turn data were obtained at Mach numbers from about 0.45 to 0.8 and are not presented herein; however, the slope values obtained from these data were used to show the variation of the various parameters over the Mach number range.

In figure 5 two sets of elevator-deflection data are presented as functions of angle of attack: the measured values shown in figure 4, and values of δ_e corrected to zero pitching acceleration to represent static trimmed-flight conditions. This correction as explained in detail in reference 5, was applied to the measured values of δ_e because the slope $d\delta_e/d\alpha$ does not indicate the true airplane static stability when relatively high pitching accelerations are obtained. Although the method used to correct the elevator-deflection data to static conditions is believed valid for low values of angle of attack, the values of the elevator pitching-effectiveness parameter $dC_m/d\delta_e$ used for this correction at high angles of attack are questionable. Therefore, the values of $\delta_{e(\ddot{\theta} = 0)}$ were plotted only over a sufficiently large range of angle of attack to show any adverse stick-fixed stability effects for the static condition.

Basic Longitudinal Stability Characteristics

Inspection of the time-history data of figure 4 shows that the rate of increase of α and C_{N_A} appears generally linear and almost proportional to the rate of increase of δ_e at the lower values of α. At moderate values of α and C_{N_A}, the rate of increase α and C_{N_A} tended to increase as the turn was further penetrated, and in most of the turns the rate of increase of δ_e also increased as the stick-force gradient and the stick force lightened. However, the relative increase in α and C_{N_A} appears greater than the increase in δ_e, thus indicating a decrease in the stick-fixed stability of the airplane, and in some instances, a pitch-up is apparent. In almost all the maneuvers, a large hinge-moment change occurred prior to attainment of the peak values of α or C_{N_A} for the maneuver (i.e., stick-free instability), which would accentuate the decrease in stick-fixed stability to the pilot. At the lower speeds, the rate change of the stick force was quite small generally and appeared slightly erratic.

These effects and others can be observed, perhaps more clearly, in figure 5 where an almost linear variation of $\delta_{e(\ddot{\theta} = 0)}$ with α (constant apparent stick-fixed static stability) is observed for the low values of α, up to 8° or 9° for Mach numbers below about 0.7, but only up to 3° or 4° for higher Mach numbers. At angles of attack above this region of constant stability, the slope of $\delta_{e(\ddot{\theta} = 0)}$ with α is reduced, indicating a reduction in stability which appeared as a pitch-up to the pilot. For convenience in identification, the angle of attack at which the reduction in stability occurred is indicated on figure 5 by the tick adjacent to the curve of $\delta_{e(\ddot{\theta} = 0)}$. In general, the reduction of stability appeared only moderatly severe at the lower speeds; about a 0.5g overshoot was reported by the pilot for maneuvers during which the control input was stopped (and subsequently reversed) when the reduction of stability was detected. At the higher speeds, however, the reduction in stability was quite severe, as shown in figures 5(i) and 5(j), and was sometimes accompanied by large pitching velocities and accelerations (for example, see fig. 5(j)). The reduction of stability appeared to exist over a limited region of α or C_{N_A}, as shown by the increase in slope of the curves of $\delta_{e(\ddot{\theta} = 0)}$ plotted against α at the higher values of α (fig. 5), indicating an increase in stick-fixed stability. Although the airplane appeared to regain stability subsequent to the pitch-up and near the peak values of C_{N_A} attained, at Mach numbers below about 0.8, the severe buffeting obviated flight in this region, so the controllability was not thoroughly investigated. In the highest Mach number maneuver performed ($M \approx 1.0$), the airplane appeared fully controllable and exhibited no apparent reduction in static stability up to the highest value of C_{N_A} (0.76) attained (fig. 5(k)). However, this effect has also been realized for other configurations of the airplane and is not attributable to the installation of wing chord-extensions on the airplane (ref. 5 and unpublished data).

At Mach numbers less than about 0.7, the stick forces exhibited a positive gradient over the low range of α and normal acceleration and almost no gradient at moderate values of α prior to a reversal of the forces at large values of α. In general, the lightening of the stick forces at moderate angles of attack tended to increase the control rate, which in turn would aggravate any pitching. At $M > 0.7$, the reversal of stick forces was rather abrupt and tended to exaggerate the severity of the pitch-up in the pilot's opinion. These results showed general agreement with those obtained on the unmodified airplane (ref. 2).

In summary, the airplane was found to be unsatisfactory for controlled accelerated flight in the region of reduced stability with chord-extensions, but appeared to retrim and regain some stability and controllability at the higher angles of attack. This latter effect, as well as the generally less abrupt changes in stick-fixed stability for the chord-extension

configuration, tended to make the airplane appear somewhat better to the pilot (but still intolerable) than the unmodified airplane. A comparison of some typical static stability data obtained with the chord-extension configuration and the unmodified airplane is shown in figure 6 to illustrate the stability changes noted by the pilot with these two configurations and the degree of improvement obtained with the chord-extensions. The pilot also thought that the airplane tended to diverge to a somewhat greater extent during the pitch-up with chord-extensions than with wing slats fully extended; however, the data shown on figure 6 do not support this opinion. In addition, the level of lift coefficients for the start of buffeting with wing chord-extensions was lowered somewhat below $M = 0.8$ (fig. 7), compared with the unmodified D-558-II airplane (ref. 11), and the pilot objected to the increase in buffeting intensity.

Boundary for the Decay in Airplane Stability

From the data shown in figures 4 and 5 (as well as from similar data which are not presented herein), the normal-force coefficient corresponding to the value of α at which the reduction in stick-fixed static stability occurs was determined for each maneuver and is presented as a function of Mach number in figure 8. It will be noted that the region between $M = 0.72$ and 0.88 is not well-defined by data points because of an elevator position transmitter malfunction during maneuvers performed at these speeds (figs. 4 and 5); nevertheless, the trend of the stability boundary is believed shown by the data points on figure 8. The value of C_{N_A} for the decay in stability decreases from about 0.75 at $M = 0.5$ to about 0.46 at $M = 0.88$, and increases to 0.55 at $M = 0.93$.

For comparative purposes, the C_{N_A}—Mach number boundary for the decay in stick-fixed stability of the unmodified airplane configuration (slats retracted and including inboard wing fences) of reference 2, corrected to $\ddot{\theta} = 0$, has been included in figure 8. As can be seen, the stability boundary for the airplane with chord-extensions is at about the same or slightly lower levels of C_{N_A} as for the unmodified airplane configuration, except at $M > 0.9$, where the boundary for the chord-extension configuration exhibits a rapid rise with increase in Mach number. This trend at $M > 0.9$ has since been exhibited with the basic clean-wing configuration, which indicated a rapid rise in the value of C_{N_A} for the stability boundary as M increased through 1.0.

Comparison of the data points for the decay in stick-fixed stability for the chord-extension configuration with the stability boundary for the slats-extended configuration (ref. 5) shows a general similarity in the trends and levels of C_{N_A} for the boundaries over the Mach number range.

Peak values of C_{N_A} obtained during the reported maneuvers are also shown in figure 8. It is felt that in some instances these peak values of C_{N_A} may correspond to maximum values of C_{N_A} attainable at the given Mach number. The data of figure 8 show that the difference between peak C_{N_A} and the stability boundary increases as M increases beyond 0.7. This would tend to increase the magnitude and potential danger of the stability problem as M increases, particularly since the decay in stability occurring at Mach numbers between about 0.8 and 0.95 is quite severe.

Comparison of Flight and Wind-Tunnel Data

In order to determine to what extent the flight data agree with the wind-tunnel data for the chord-extension configuration on the D-558-II airplane, comparisons of flight and tunnel data in terms of the airplane pitching-moment coefficient C_m, are presented in figure 9. These data also make feasible an evaluation of the wind-tunnel data and the improvement in stability exhibited in tunnel studies for wing chord-extensions compared with the unmodified airplane. (See fig. 10.) The wind-tunnel data of figure 9 were obtained during tests in the Langley high-speed 7- by 10-foot tunnel of a model of the D-558-II airplane equipped with wing chord-extensions similar to those tested on the airplane (unpublished data). The flight data were calculated using the data of figures 4(c) and 5(c) (for the comparison at $M = 0.6$) and the data of figures 4(i) and 5(i) (for the comparison at $M = 0.89$), as well as unpublished flight data, by an analysis similar to that employed in reference 12. Fairly good agreement is shown in figure 9 for the flight and wind-tunnel data, except at the higher angles of attack at $M = 0.89$, in which region the values of some of the parameters employed in the flight calculations may be questionable. Of particular significance is the agreement shown in the trends of the curves over the angle-of-attack range, particularly the decreases in stability evident at moderate angles of attack. Wind-tunnel studies (refs. 6, 7, and unpublished data) shown in figures 9 and 10, indicated the appreciable unstable characteristics of the unmodified airplane occurring at moderate values of α were generally altered to regions of neutral or slightly positive stability with the addition of the subject chord-extensions. However, pitch-ups were encountered with both configurations in flight tests. This fact, coupled with the dynamic character of an accelerated longitudinal maneuver, including inertia effects, would indicate that abrupt reductions in stability could tend to cause pitch-up and are not tolerable for controlled flight. Of course, as discussed in the INTRODUCTION, dynamic effects and other phenomena must be considered in analyzing wind-tunnel data in terms of airplane handling qualities, as outlined in reference 8.

Subsequent to the performance of the subject flight investigation, methods of analysis were formulated to calculate the response of an airplane to longitudinal control input, using wind-tunnel pitching-moment data (ref. 8). In order to determine to what extent the decrease in stability and the pitch-up could be predicted from wind-tunnel data, calculations were made of the airplane response and are compared in figure 11 with the measured airplane response for a Mach number of about 0.6. The flight data are the same as presented in figure 4(c). The calculated time history was computed by the method of reference 8, starting at 9.0 seconds, by using the C_m data of figure 10 (for the chord-extension configuration) and other unpublished data. For case A, in which the actual elevator input was used, the calculated airplane response indicated an earlier increase in the rate of airplane response (decrease in stability and subsequent pitch-up) than was obtained in flight. Figure 9 shows that this results from the slightly lower value of α for the decrease in stability that was exhibited in the wind-tunnel data than for flight data. The calculated data for case A (fig. 11) show that the pitch-up was followed by a tendency to recover, starting at about time 14.5 seconds, as the airplane regains some stability (see fig. 10). Subsequently, the increased rate of elevator input after time 16 seconds pitches the airplane to higher values of α, and it appears that the calculated maximum α would approach the actual value attained. Inasmuch as the wind-tunnel data of figure 9 showed that the decrease in stability occurred at a slightly lower value of α than in flight, it was thought resonable to assume for some calculations an increased rate of control input, starting approximately at the wind-tunnel value of α for the decay in stability, similar to the increased control rate used in flight after the actual decay in stability. This control input is shown as case B, for which an increase in the rate of airplane response over that provided in case A was obtained; and the calculated rate of response is similar to that measured in flight, but the peak value of α is less. By increasing the maximum assumed control input in case B to that used in flight (giving case C), the calculated peak value of α as well as the response rate is similar to that measured in flight. It therefore appears that fairly accurate calculations of airplane response to longitudinal control input can be made from wind-tunnel data by means of the method of reference 8.

Stability Parameters

Variation of $d\delta_e/dC_{N_A}$ and dF_e/dn with Mach number.- Variations with Mach number of the apparent airplane stability parameter $d\delta_e/dC_{N_A}$ and the elevator control force parameter dF_e/dn, measured in the stable region, are shown in figure 12. At the forward center-of-gravity positions, the values of $d\delta_e/dC_{N_A}$ and dF_e/dn are substantially constant at about

10 and $13\frac{1}{2}$, respectively, for Mach numbers up to about 0.65. At $M \gtrapprox 0.65$, the values of both parameters increased rapidly with increase in Mach number, and at $M = 1.005$, $d\delta_e/dC_{N_A} \approx 43$ and $dF_e/dn \approx 115$. As was discussed in reference 1 for the airplane configuration incorporating inboard fences on the unmodified wing, most of the increase in $d\delta_e/dC_{N_A}$ and dF_e/dn at Mach numbers below about 0.85 may be attributed to an increase in the stability of the airplane, inasmuch as the elevator effectiveness does not change much in this range. At $M \gtrapprox 0.85$, however, unpublished data indicate a large decrease in elevator effectiveness as M increases; therefore, the increases noted at $M \gtrapprox 0.85$ in the values of the parameters on figure 12 probably result from both an increase in airplane stability and a decrease in elevator effectiveness.

The values of $d\delta_e/dC_{N_A}$ shown on figure 12 for the chord-extension configuration at the rearward center-of-gravity location (28.0 to 28.2 percent M.A.C.) are for a limited Mach number range and exhibit almost a constant decrement over this range compared to the values for the forward center-of-gravity location. Cross plots of the values of $d\delta_e/dC_{N_A}$ against the actual values of center-of-gravity location for maneuvers at comparable speeds show that the stick-fixed maneuver point for the airplane with chord-extensions is located at about 47 percent mean aerodynamic chord for Mach numbers between 0.5 and 0.7.

For comparison, the curves of $d\delta_e/dC_{N_A}$ and dF_e/dn for the unmodified airplane (ref. 13) are also shown in figure 12, and show the same trends with increase in Mach number as do the curves for the airplane with chord-extensions. The similarity in the curves and values of $d\delta_e/dC_{N_A}$ for the two configurations, in spite of different center-of-gravity locations, would be expected, as explained previously, because the wind-tunnel data of references 6 and 7 and unpublished data show that the airplane would have less stability with chord-extensions than in the unmodified configuration for similar center-of-gravity locations. Consequently, the forward center-of-gravity locations tested with chord-extensions were chosen to provide the same stability as the unmodified airplane having its center of gravity at about 26 to 27 percent mean aerodynamic chord. Therefore, it may readily be seen that addition of wing chord-extensions caused the airplane stick-fixed neutral point to move forward about $0.03\bar{c}$. The almost constant difference in dF_e/dn (about 3 lb/g) noted at the lower Mach numbers for the two configurations is somewhat unexpected, in view of the agreement in the values of $d\delta_e/dC_{N_A}$, and is unexplainable without further detailed tests.

Variation of $dC_{N_A}/d\alpha$ with Mach number.- The variation of the airplane normal-force-coefficient-curve slope with Mach number for the airplane with chord-extensions is shown in figure 13. The values of

$dC_{N_A}/d\alpha$ increase from about 0.066 to about 0.093 at Mach numbers of 0.45 and 0.94, respectively, then decrease to about 0.090 at a Mach number of 1.005. The comparable curve for the unmodified airplane (with only inboard fences on the wings), originally presented in reference 14, is included in figure 13. The two configurations exhibit the same trends over the Mach number range, and the values of $dC_{N_A}/d\alpha$ are in fairly good agreement. It might be anticipated that the values of $dC_{N_A}/d\alpha$ for the chord-extension configuration would be slightly higher than for the unmodified airplane, inasmuch as the chord-extensions increased the wing area about $3\frac{1}{2}$ percent, whereas the values of C_{N_A} were based on the original wing area. However, this result was not realized within the accuracy of the data, possibly because separated flow off the chord-extension may have cancelled the effects of increased wing area.

CONCLUSIONS

Results of a longitudinal stability investigation at subsonic and transonic speeds of the swept-wing Douglas D-558-II research airplane, modified to include 0.32-semispan wing leading-edge chord-extensions with wing fences removed, led to the following conclusions:

1. Addition of wing chord-extensions had only a minor effect on the decay in stick-fixed stability (pitch-up) and stick-free stability experienced by the airplane at moderate angles of attack. The chord-extensions alleviated the pitch-up to a small degree, but the pilot still considered the airplane unsatisfactory for controlled accelerated flight in this region. However, at the higher angles of attack, the airplane appeared to retrim and regain some stability.

2. The normal-force coefficient at which the decay in stick-fixed stability occurred decreased from a value of about 0.75 at a Mach number of 0.5 to about 0.46 at a Mach number of 0.88, and then increased to about 0.55 at a Mach number of 0.93. A value of normal-force coefficient of 0.76 was attained at a Mach number of 0.98 with no apparent reduction in stability.

3. The buffeting of the airplane was of such a nature that the increase in buffeting intensity induced by the chord-extensions became a major problem, in addition to the longitudinal instability problem.

4. A comparison of wind-tunnel with flight data showed good agreement in the reduction of stability evident at moderate angles of attack. The results indicated that an abrupt reduction of stability, to a region of neutral or even slight stability, could tend to cause pitch-up.

Subsequent to the performance of the subject flight investigation, an analytical method (RM L53I02) was formulated to calculate airplane response to longitudinal control input, using wind-tunnel data. Comparison of results obtained by this method appeared to give fairly accurate correlation with flight results.

5. At low lift coefficients, the trends in the values of the apparent stability parameter $d\delta_e/dC_{N_A}$ and the elevator control force parameter dF_e/dn were little affected by the addition of wing chord-extensions; the values of $d\delta_e/dC_{N_A}$ increasing approximately fourfold as Mach number was increased from about 0.5 to 1.005, and dF_e/dn increasing about ninefold in the same Mach number range. However, addition of the wing chord-extensions caused the airplane stick-fixed neutral point to move forward about 3 percent mean aerodynamic chord.

6. The airplane normal-force-coefficient-curve slope $dC_{N_A}/d\alpha$ was little affected by the addition of the chord-extension. The values increased from about 0.066 to about 0.093 at Mach numbers of 0.45 and 0.94, respectively, then decreased to about 0.090 at a Mach number of 1.005.

High-Speed Flight Station,
National Advisory Committee for Aeronautics,
Edwards, Calif., August 2, 1954.

REFERENCES

1. Sjoberg, S. A., Peele, James R., and Griffith, John H.: Flight Measurements With the Douglas D-558-II (BuAero No. 37974) Research Airplane. Static Longitudinal Stability and Control Characteristics at Mach Numbers up to 0.87. NACA RM L50K13, 1951.

2. Fischel, Jack, and Nugent, Jack: Flight Determination of the Longitudinal Stability in Accelerated Maneuvers at Transonic Speeds for the Douglas D-558-II Research Airplane Including the Effects of an Outboard Wing Fence. NACA RM L53A16, 1953.

3. Anderson, Seth B., and Bray, Richard S.: A Flight Evaluation of the Longitudinal Stability Characteristics Associated With the Pitch-Up of a Swept-Wing Airplane in Maneuvering Flight at Transonic Speeds. NACA RM A51I12, 1951.

4. McFadden, Norman M., Rathert, George A., Jr., and Bray, Richard S.: The Effectiveness of Wing Vortex Generators in Improving the Maneuvering Characteristics of a Swept-Wing Airplane at Transonic Speeds. NACA RM A51J18, 1952.

5. Fischel, Jack: Effect of Wing Slats and Inboard Wing Fences on the Longitudinal Stability Characteristics of the Douglas D-558-II Research Airplane in Accelerated Maneuvers at Subsonic and Transonic Speeds. NACA RM L53L16, 1954.

6. Jaquet, Bryon M.: Effects of Chord Discontinuities and Chordwise Fences on Low-Speed Static Longitudinal Stability of an Airplane Model Having a 35° Sweptback Wing. NACA RM L52C25, 1952.

7. Jaquet, Bryon M.: Effects of Chord-Extension and Droop of Combined Leading-Edge Flap and Chord-Extension on Low-Speed Static Longitudinal Stability Characteristics of an Airplane Model Having 35° Sweptback Wing With Plain Flaps Neutral or Deflected. NACA RM L52K21a, 1953.

8. Campbell, George S., and Weil, Joseph: The Interpretation of Nonlinear Pitching Moments in Relation to the Pitch-Up Problem. NACA RM L53I02, 1953.

9. Gracey, William, Letko, William, and Russell, Walter R.: Wind-Tunnel Investigation of a Number of Total-Pressure Tubes at High Angles of Attack - Subsonic Speeds. NACA TN 2331, 1951. (Supersedes NACA RM L50G19.)

10. Zalovcik, John A.: A Radar Method of Calibrating Airspeed Installations on Airplanes in Maneuvers at High Altitudes and at Transonic and Supersonic Speeds. NACA Rep. 985, 1950. (Supersedes NACA TN 1979.)

11. Baker, Thomas F.: Some Measurements of Buffeting Encountered by a Douglas D-558-II Research Airplane in the Mach Number Range From 0.5 to 0.95. NACA RM L53I17, 1953.

12. Peck, Robert F., and Mitchell, Jesse L.: Rocket-Model Investigation of Longitudinal Stability and Drag Characteristics of an Airplane Configuration Having a 60° Delta Wing and a High Unswept Horizontal Tail. NACA RM L52K04a, 1953.

13. Williams, W. C., and Crossfield, A. S.: Handling Qualities of High-Speed Airplanes. NACA RM L52A08, 1952.

14. Mayer, John P., Valentine, George M., and Swanson, Beverly J.: Flight Measurements With the Douglas D-558-II (BuAero No. 37974) Research Airplane. Measurements of Wing Loads at Mach Numbers up to 0.87. NACA RM L50H16, 1950.

TABLE I.- PHYSICAL CHARACTERISTICS OF THE UNMODIFIED DOUGLAS D-558-II AIRPLANE

Wing:	
Root airfoil section (normal to 0.30 chord of unswept panel)	NACA 63-010
Tip airfoil section (normal to 0.30 chord of unswept panel)	NACA 63_1-012
Total area, sq ft	175.0
Span, ft	25.0
Mean aerodynamic chord, in.	87.301
Root chord (parallel to plane of symmetry), in.	108.51
Tip chord (parallel to plane of symmetry), in.	61.18
Taper ratio	0.565
Aspect ratio	3.570
Sweep at 0.30 chord of unswept panel, deg	35.0
Sweep of leading edge, deg	38.8
Incidence at fuselage center line, deg	3.0
Dihedral, deg	-3.0
Geometric twist, deg	0
Total aileron area (rearward of hinge line), sq ft	9.8
Aileron travel (each), deg	±15
Total flap area, sq ft	12.58
Flap travel, deg	50
Horizontal tail:	
Root airfoil section (normal to 0.30 chord of unswept panel)	NACA 63-010
Tip airfoil section (normal to 0.30 chord of unswept panel)	NACA 63-010
Area (including fuselage), sq ft	39.9
Span, in.	143.6
Mean aerodynamic chord, in.	41.75
Root chord (parallel to plane of symmetry), in.	53.6
Tip chord (parallel to plane of symmetry), in.	26.8
Taper ratio	0.50
Aspect ratio	3.59
Sweep at 0.30 chord line of unswept panel, deg	40.0
Dihedral, deg	0
Elevator area, sq ft	9.4
Elevator travel, deg	
Up	25
Down	15
Stabilizer travel, deg	
Leading edge up	4
Leading edge down	5
Vertical tail:	
Airfoil section (normal to 0.30 chord of unswept panel)	NACA 63-010
Area, sq ft	36.6
Height from fuselage center line, in.	98.0
Root chord (parallel to fuselage center line), in.	146.0
Tip chord (parallel to fuselage center line), in.	44.0
Sweep angle at 0.30 chord of unswept panel, deg	49.0
Rudder area (rearward of hinge line), sq ft	6.15
Rudder travel, deg	±25
Fuselage:	
Length, ft	42.0
Maximum diameter, in.	60.0
Fineness ratio	8.40
Speed-retarder area, sq ft	5.25
Engines:	
Turbojet	J-34-WE-40
Rocket	LR8-RM-6
Airplane weight, lb:	
Full jet and rocket fuel	15,570
Full jet fuel	12,382
No fuel	10,822

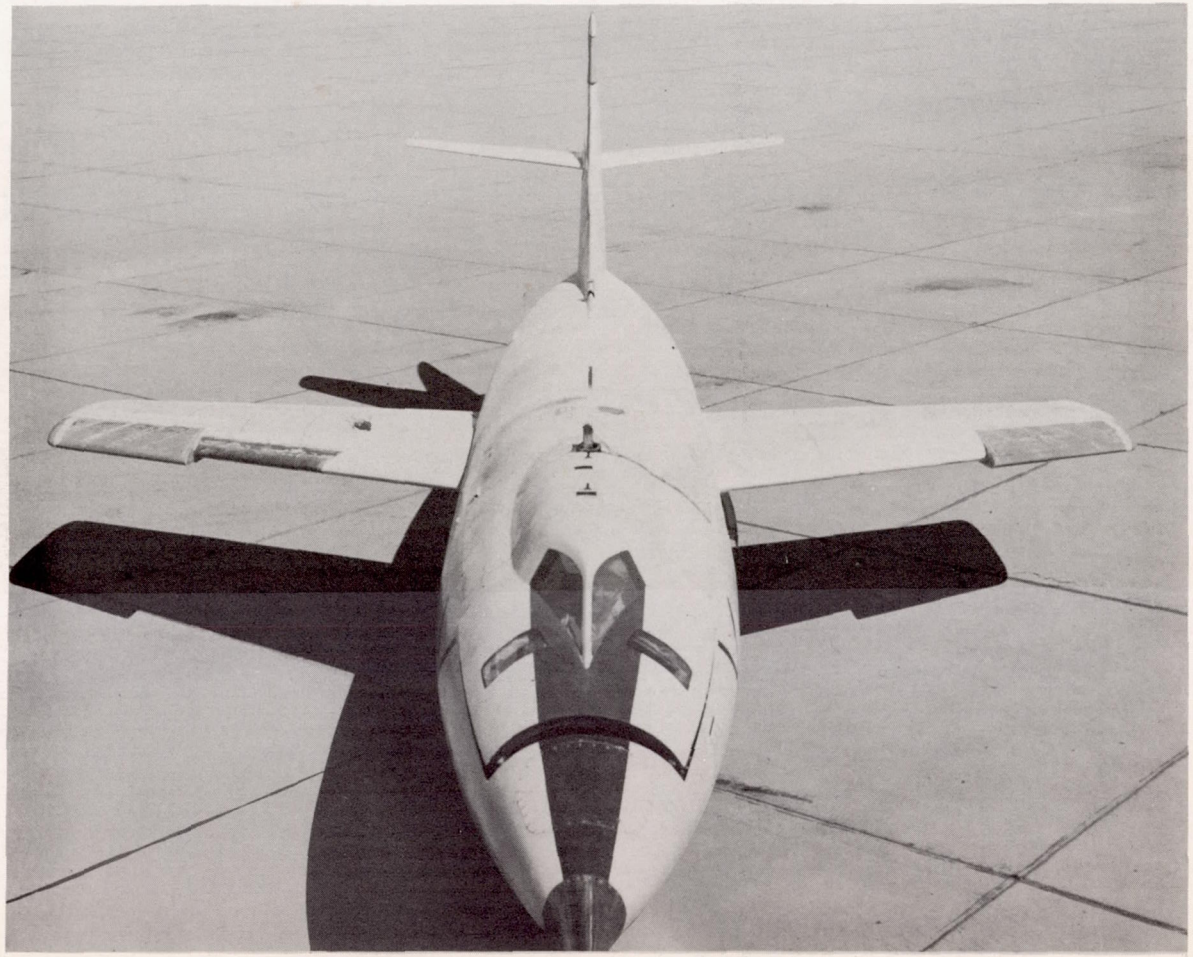

L-85622

(a) Overhead front view.

Figure 1.- Photographs of the Douglas D-558-II research airplane showing the wing leading-edge chord-extensions.

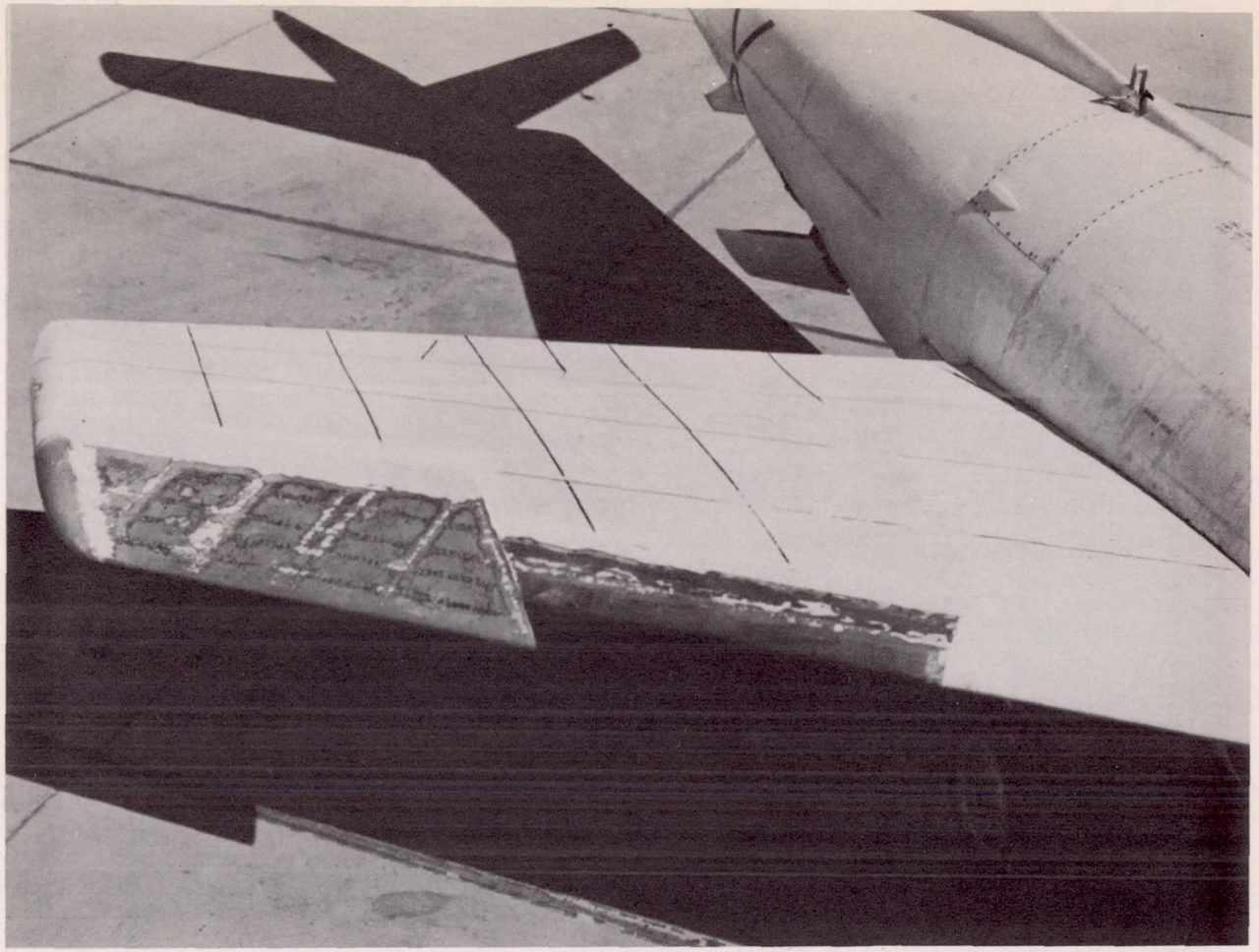

L-85623

(b) Three-quarter front view of the right wing.

Figure 1.- Concluded.

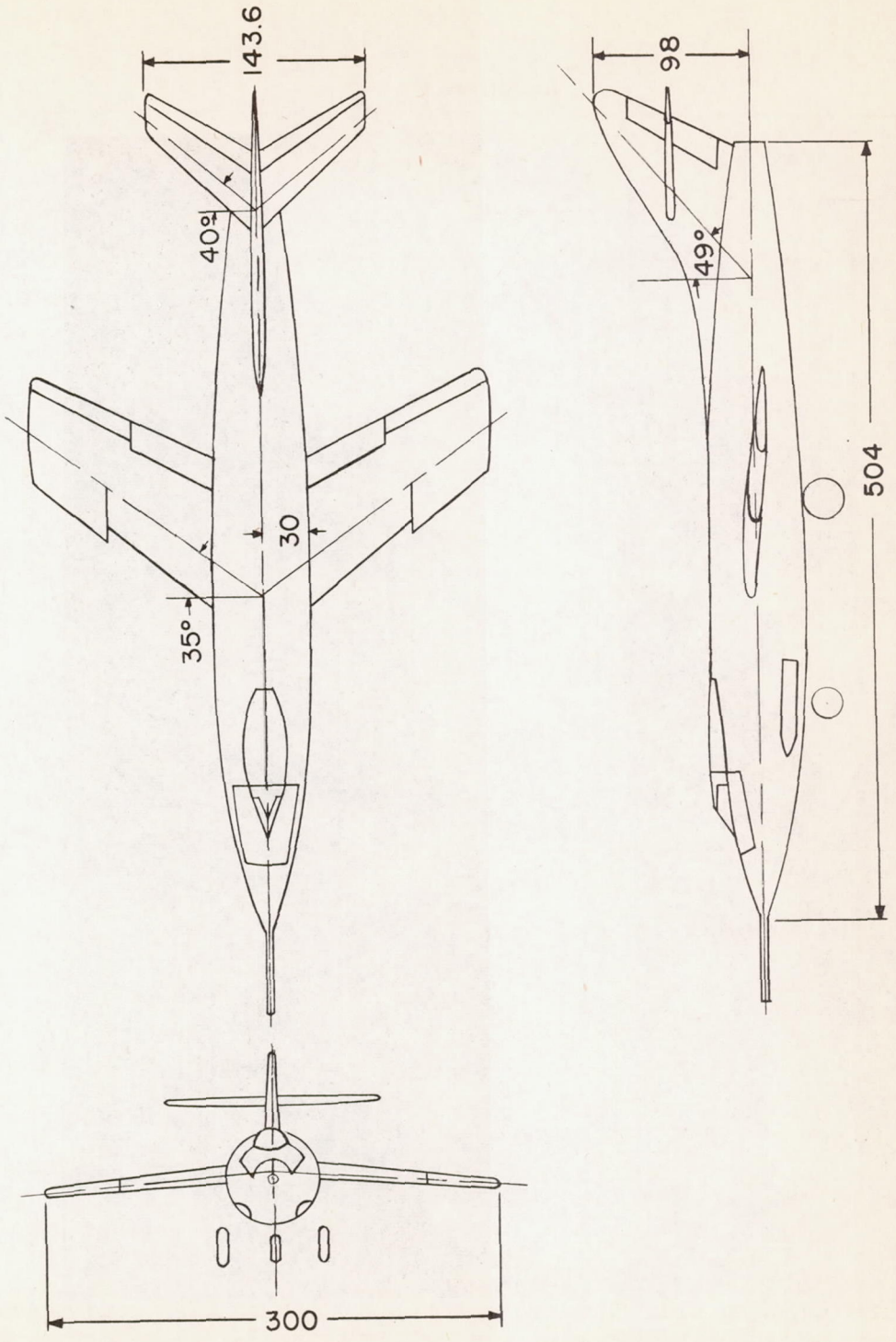

Figure 2.- Three-view drawing of the Douglas D-558-II research airplane equipped with wing leading-edge chord-extensions. Dimensions given in inches unless otherwise noted.

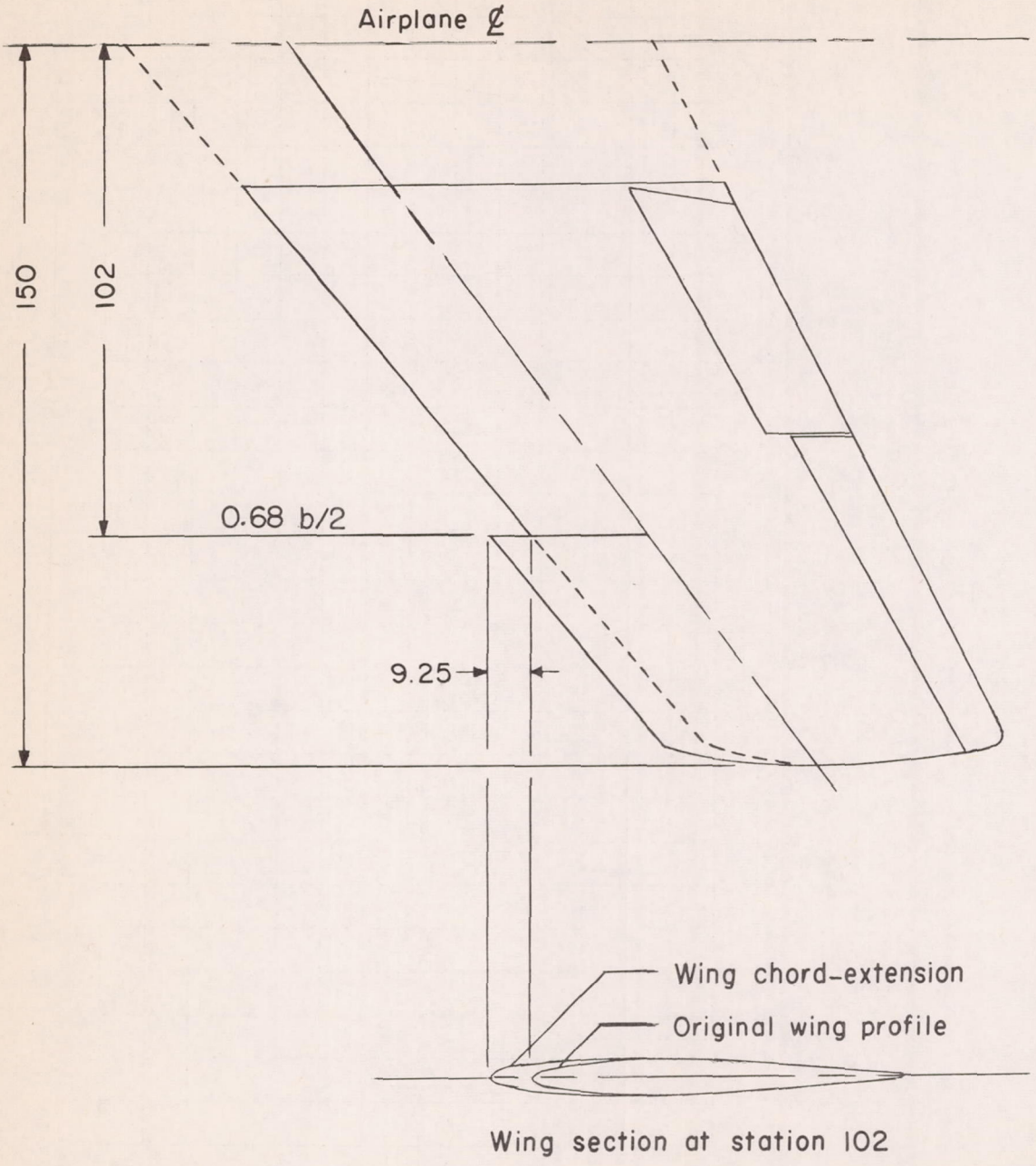

Figure 3.- Wing plan form and profile section showing leading-edge chord-extensions on the Douglas D-558-II research airplane. Dimensions given in inches unless otherwise noted.

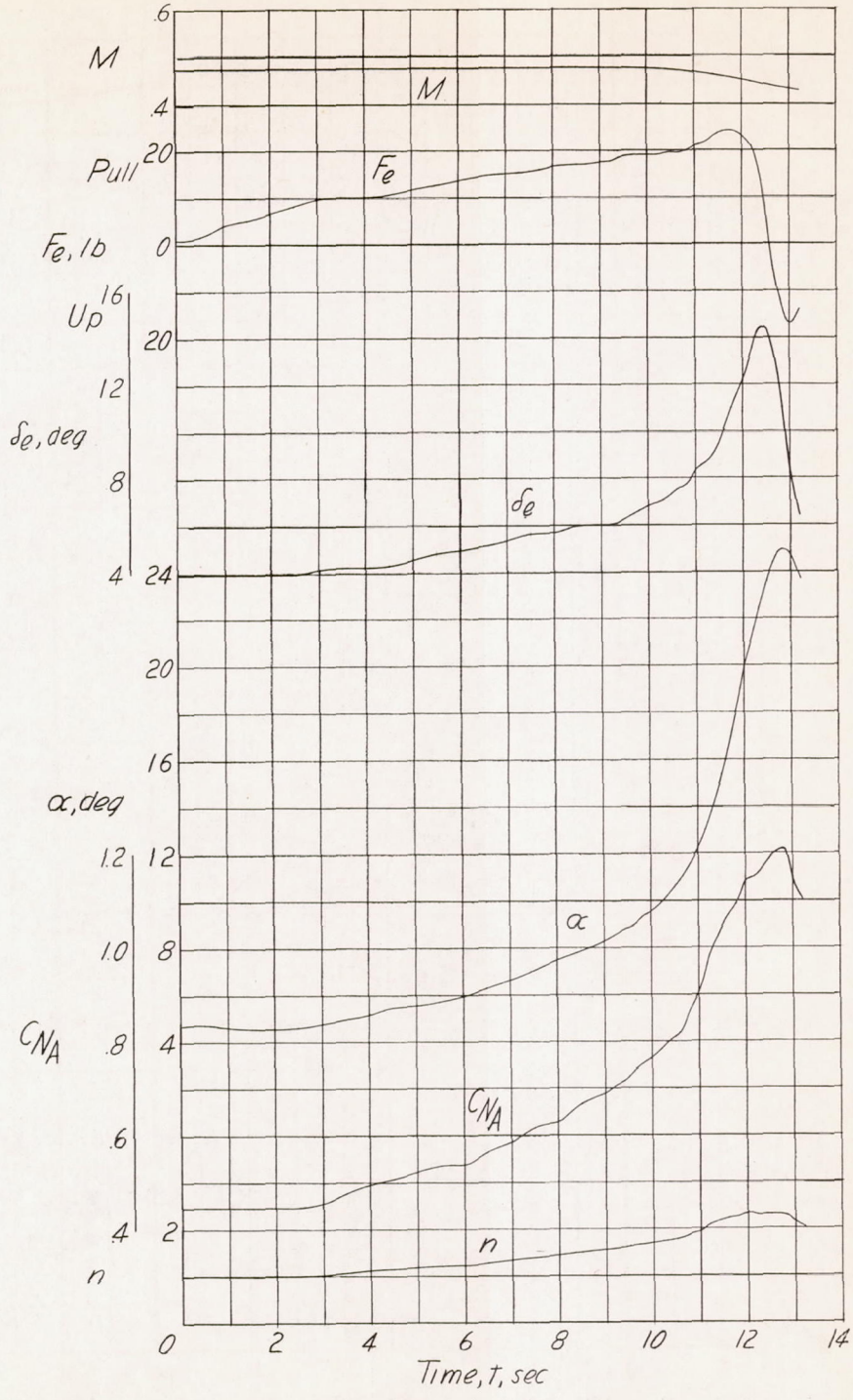

(a) $h_p \approx 20{,}100$ feet; $i_t = 1.6^\circ$; center of gravity at 22.8 percent mean aerodynamic chord.

Figure 4.- Time histories of wind-up turns performed by the Douglas D-558-II research airplane equipped with wing chord-extensions.

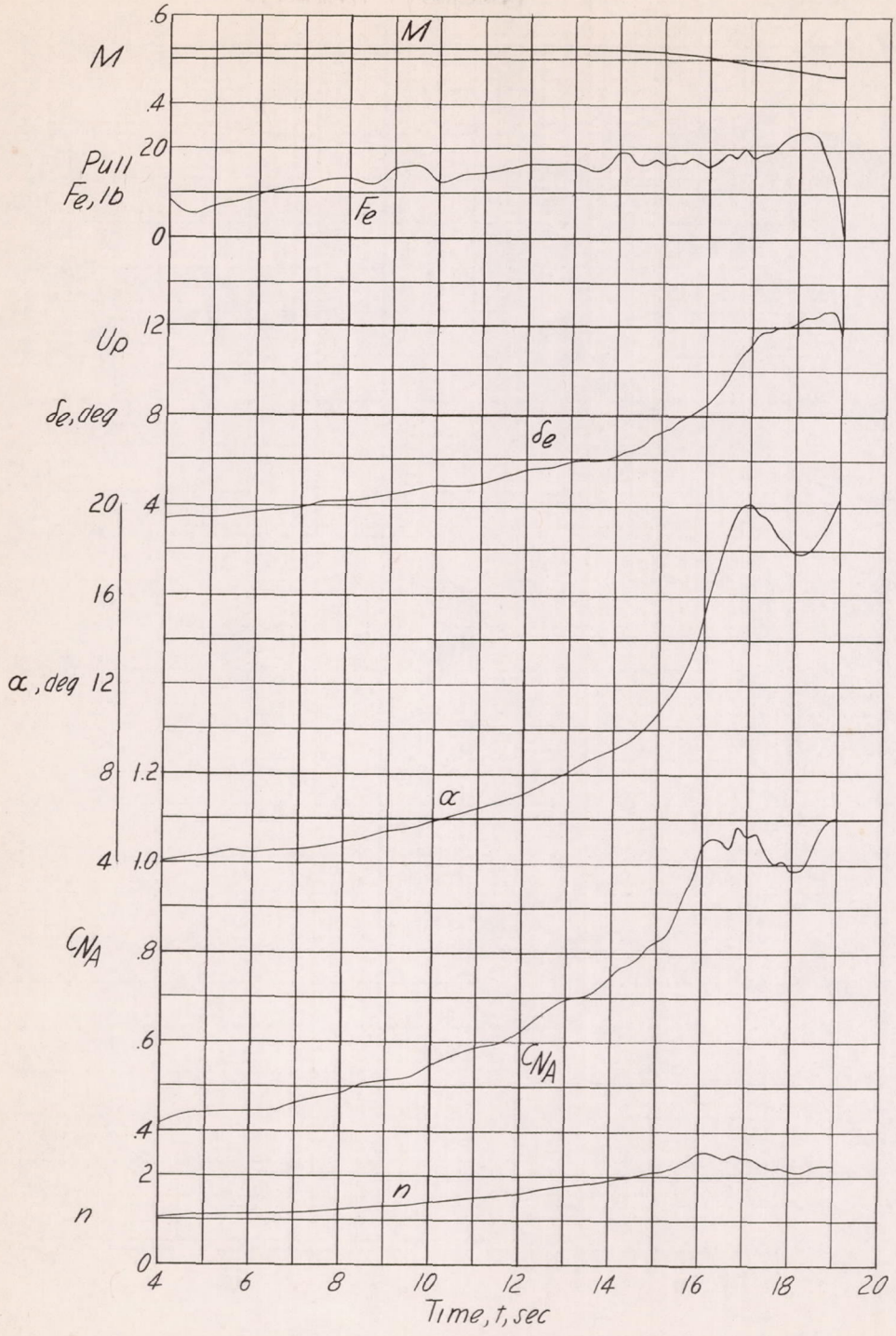

(b) $h_p \approx 21{,}600$ feet; $i_t = 1.6^\circ$; center of gravity at 22.8 percent mean aerodynamic chord.

Figure 4.- Continued.

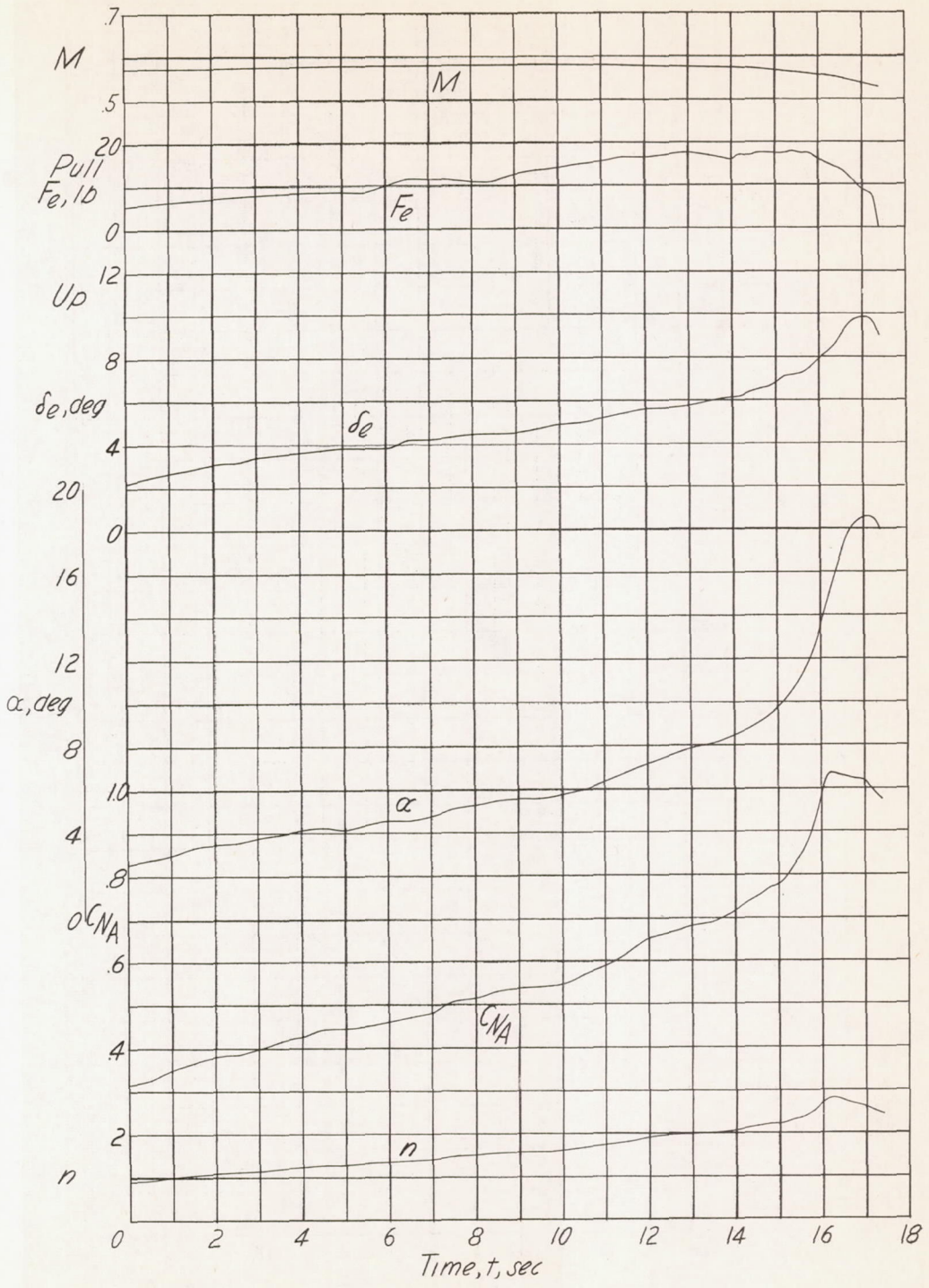

(c) $h_p \approx 22{,}800$ feet; $i_t = 1.6^\circ$; center of gravity at 22.7 percent mean aerodynamic chord.

Figure 4.- Continued.

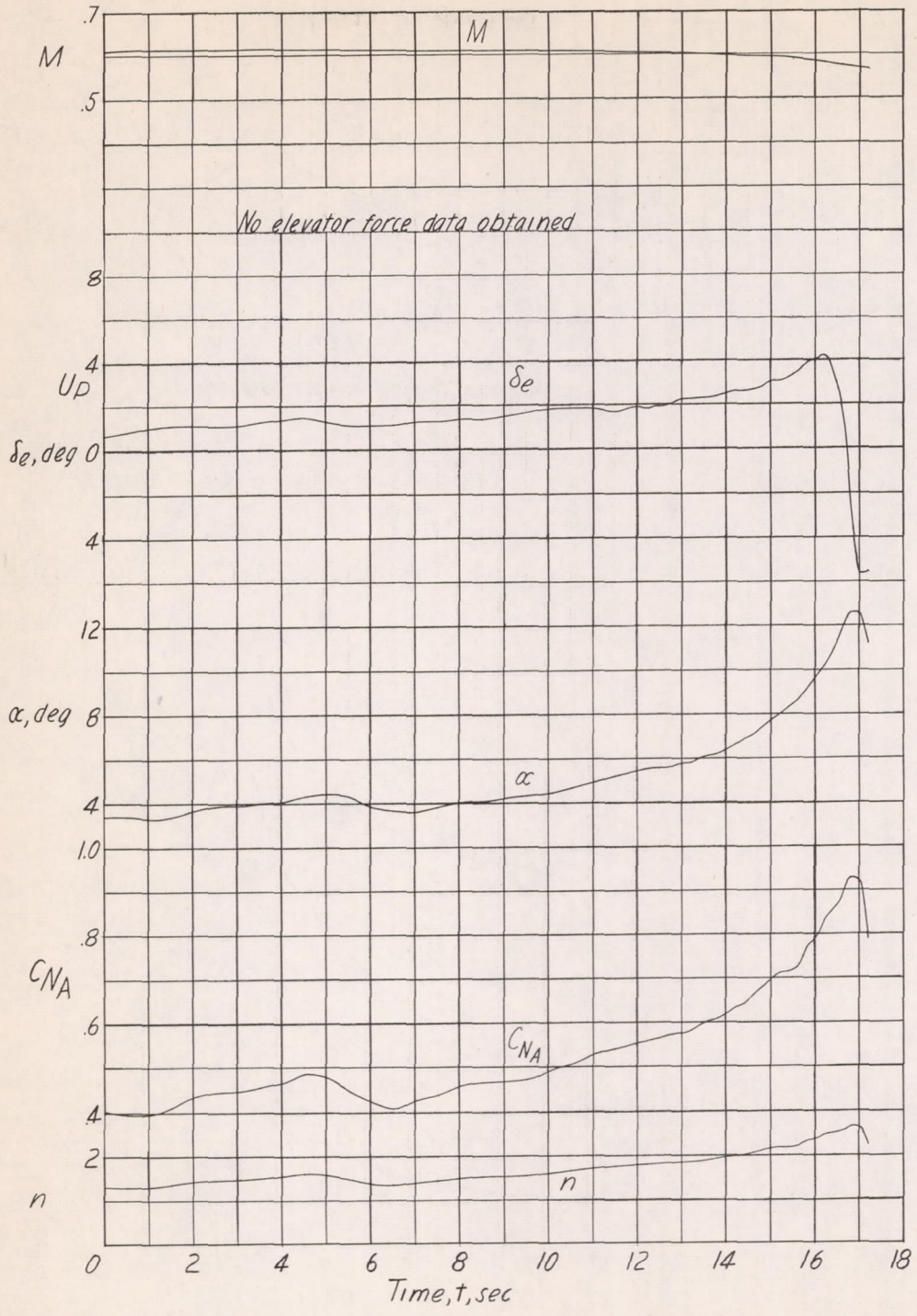

(d) $h_p \approx 24{,}100$ feet; $i_t = 1.3^\circ$; center of gravity at 28.0 percent mean aerodynamic chord.

Figure 4.- Continued.

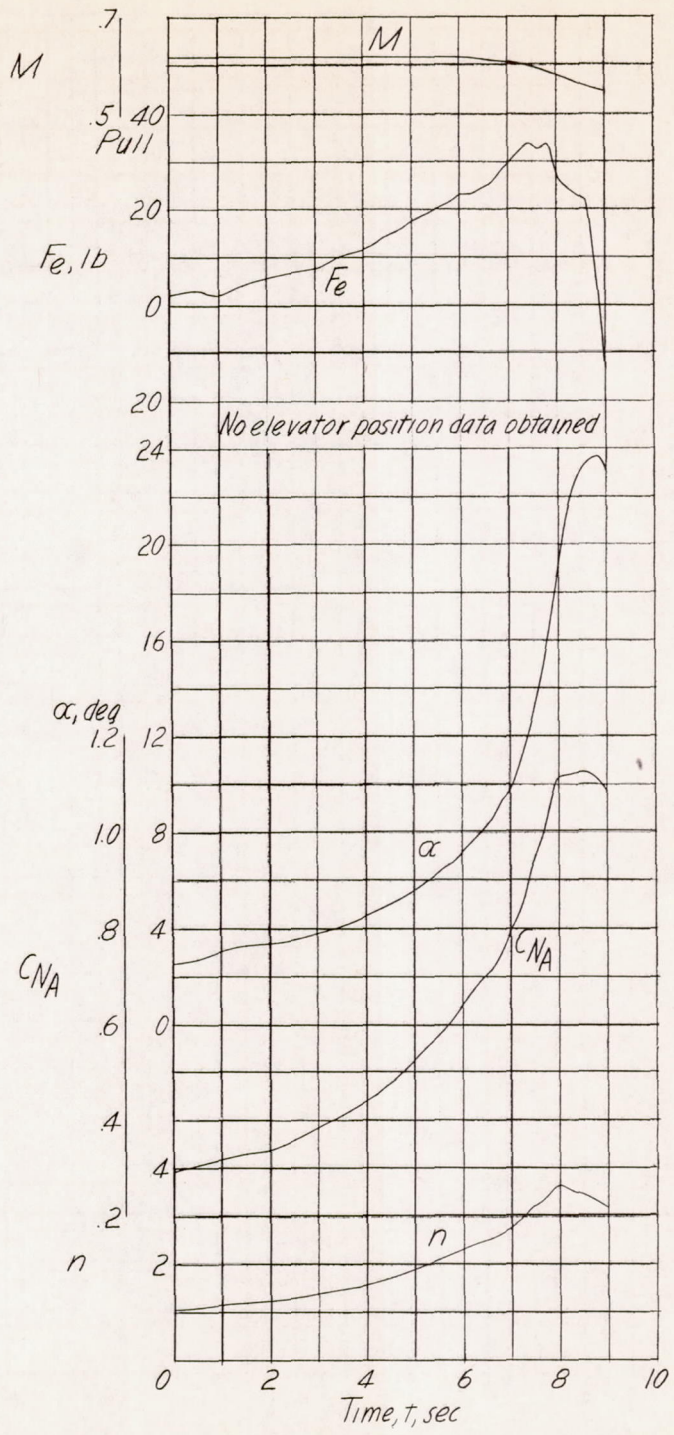

(e) $h_p \approx 21{,}500$ feet; $i_t = 1.7°$; center of gravity at 24.1 percent mean aerodynamic chord.

Figure 4.- Continued.

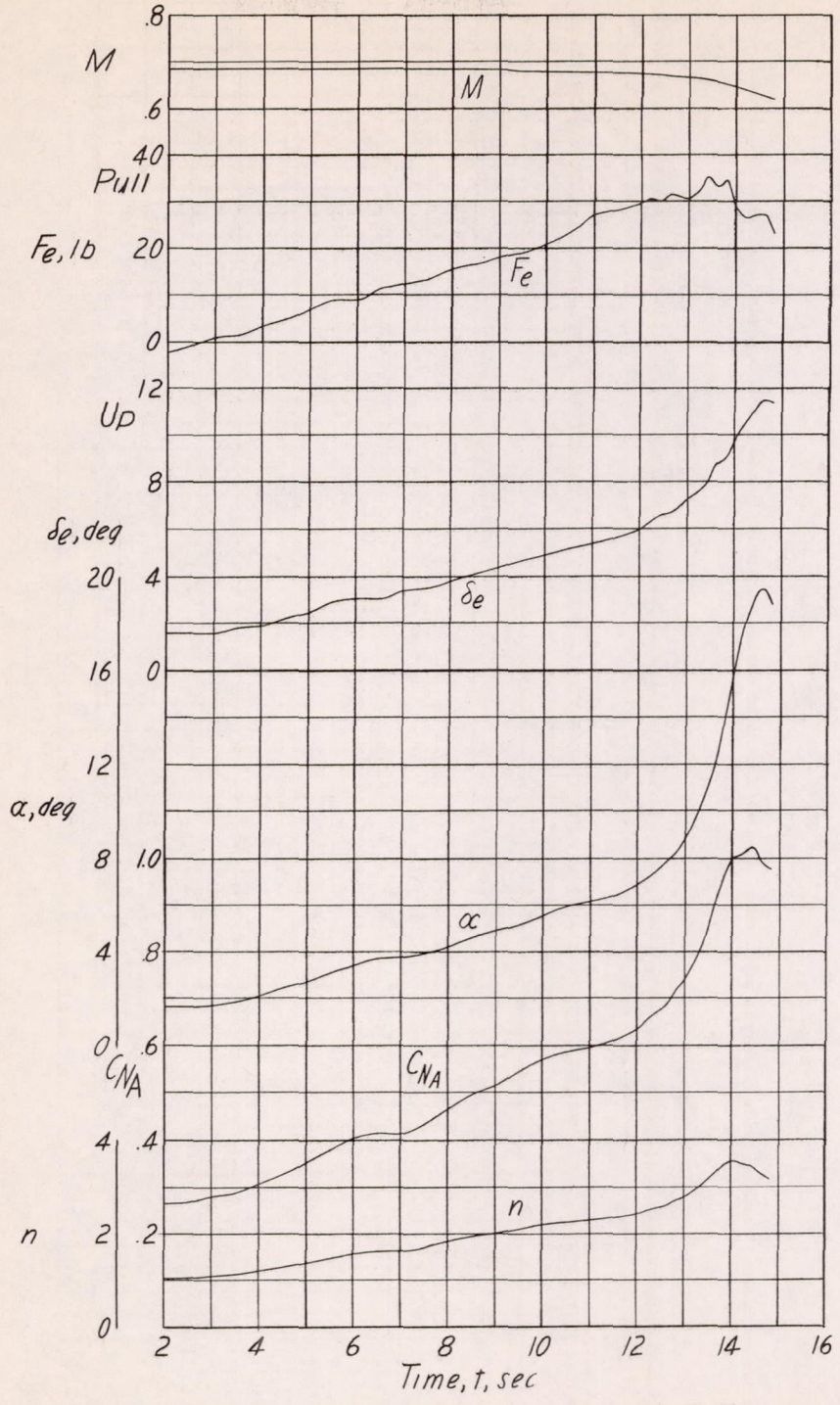

(f) $h_p \approx 23{,}500$ feet; $i_t = 1.7°$; center of gravity at 24.1 percent mean aerodynamic chord.

Figure 4.- Continued.

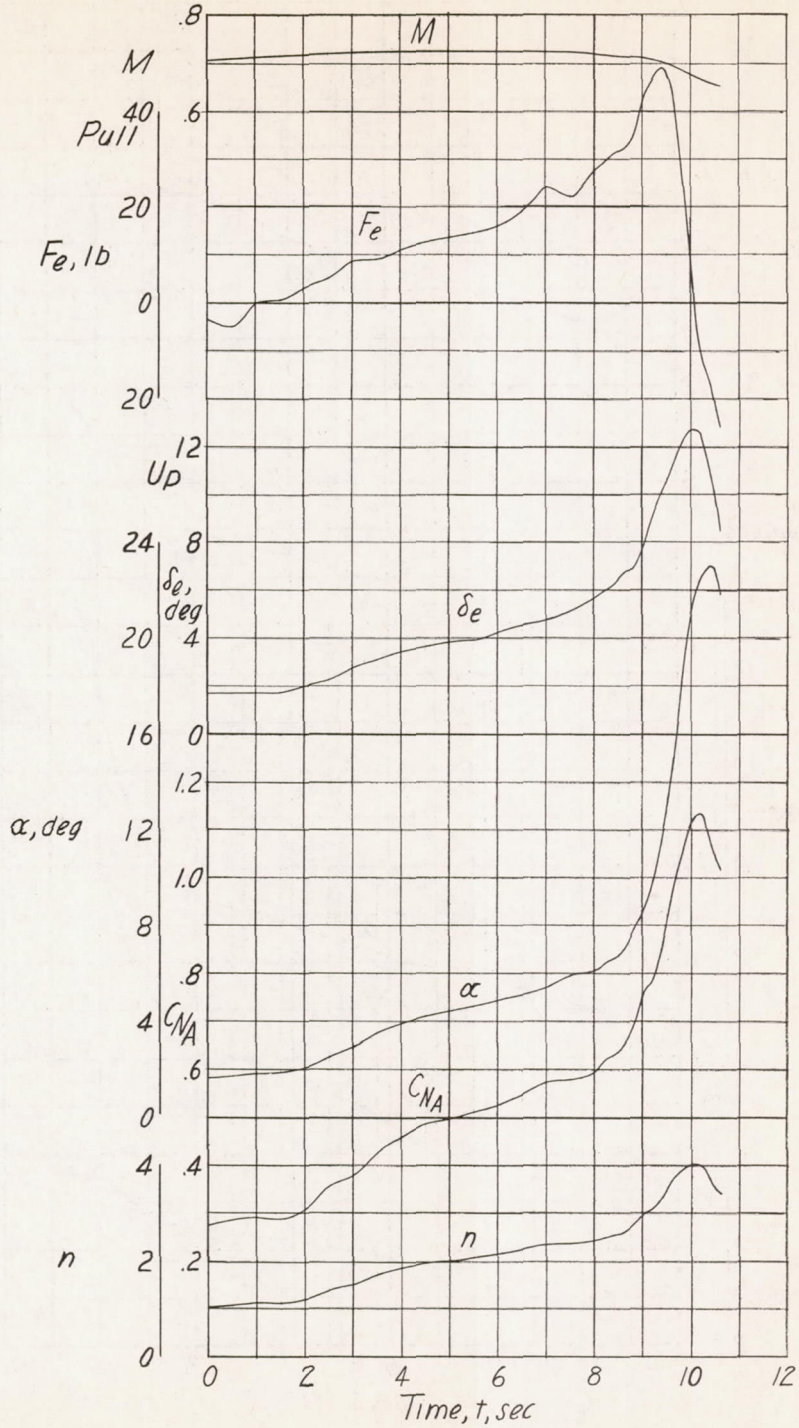

(g) $h_p \approx 25{,}300$ feet; $i_t = 1.6^\circ$; center of gravity at 22.6 percent mean aerodynamic chord.

Figure 4.- Continued.

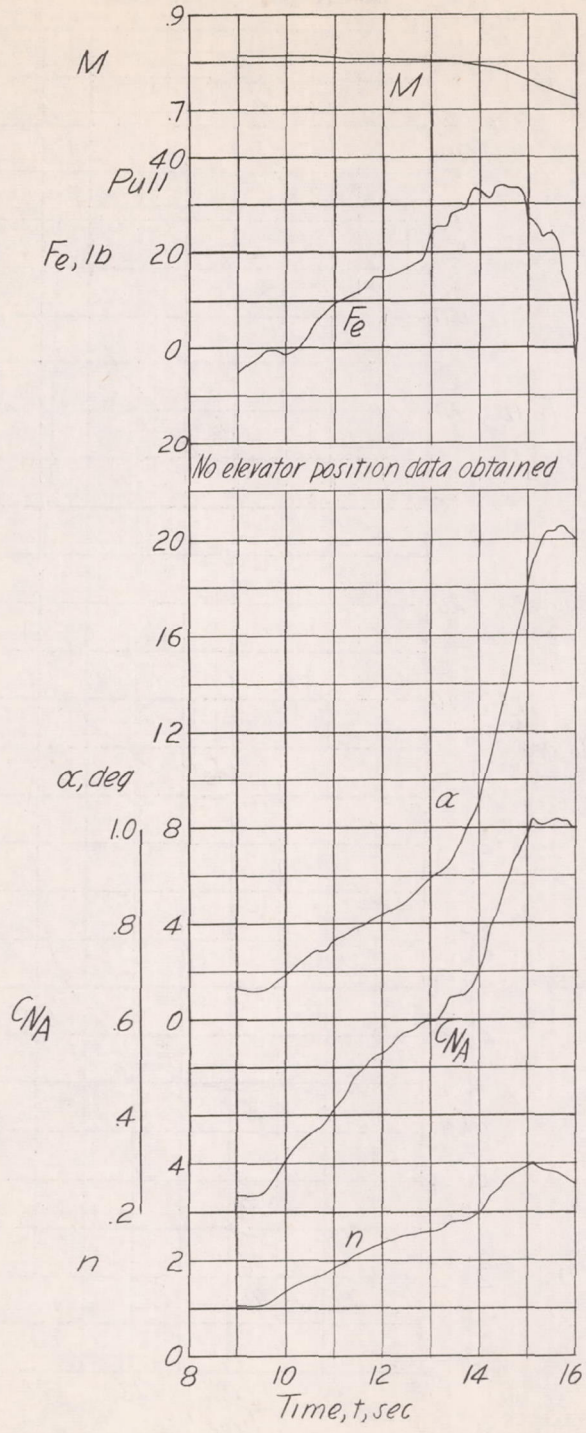

(h) $h_p \approx 28{,}900$ feet; $i_t = 1.7°$; center of gravity at 24.1 percent mean aerodynamic chord.

Figure 4.- Continued.

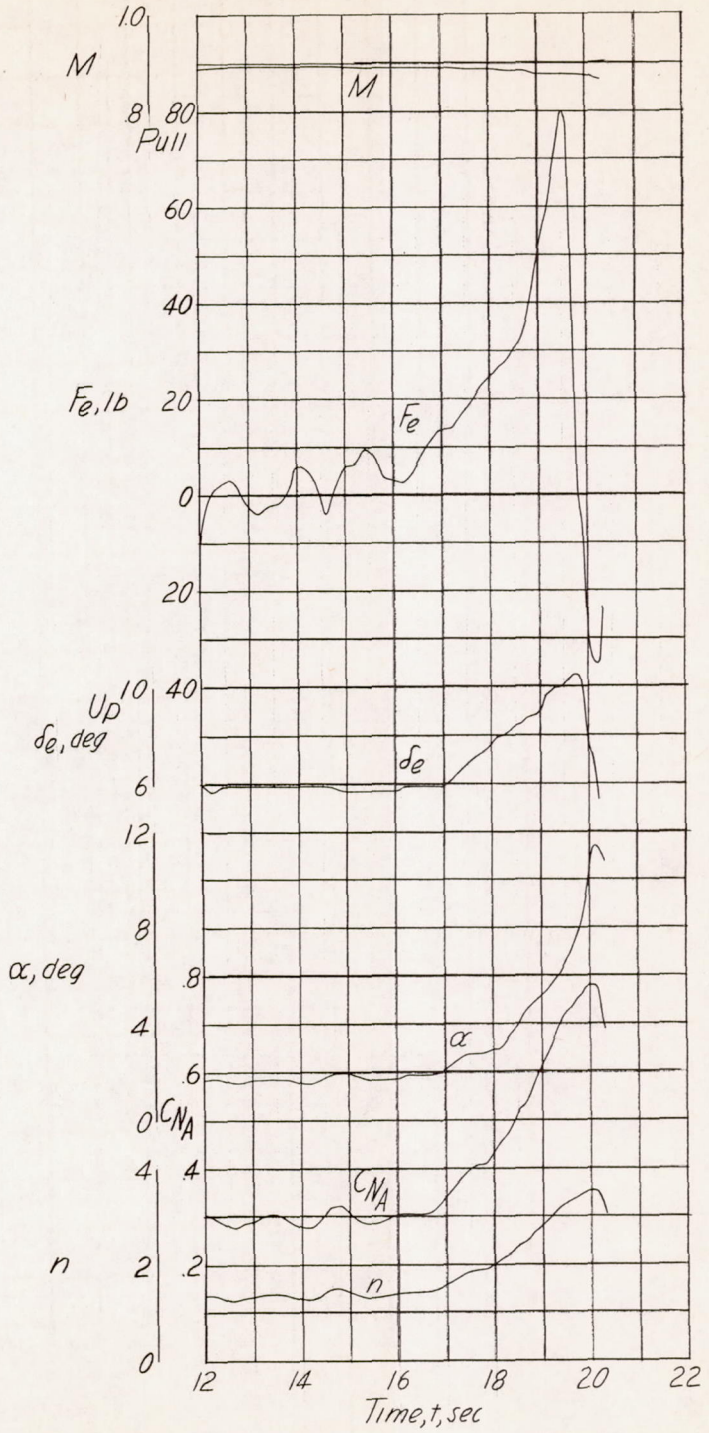

(i) $h_p \approx 30{,}800$ feet; $i_t = 1.7^\circ$; center of gravity at 24.7 percent mean aerodynamic chord.

Figure 4.- Continued.

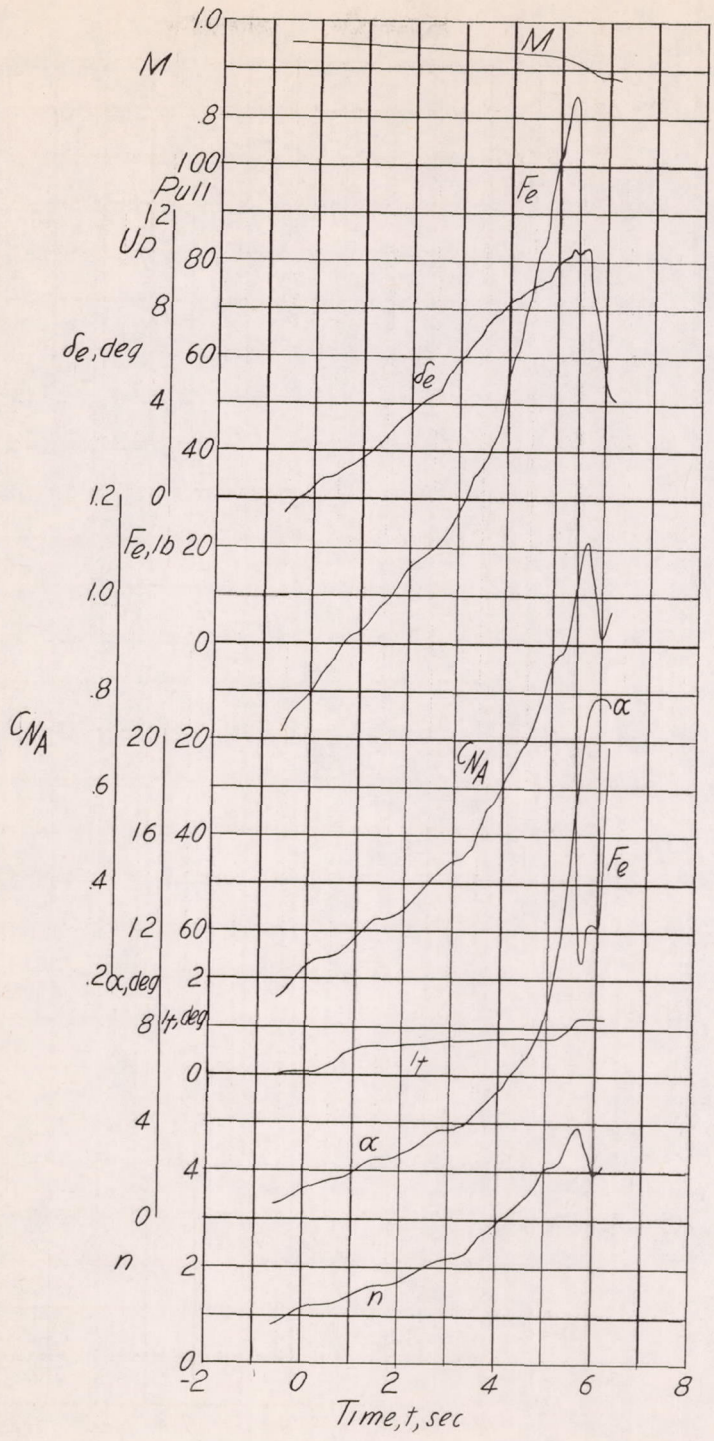

(j) $h_p \approx 32{,}000$ feet; center of gravity at 24.6 percent mean aerodynamic chord.

Figure 4.- Continued.

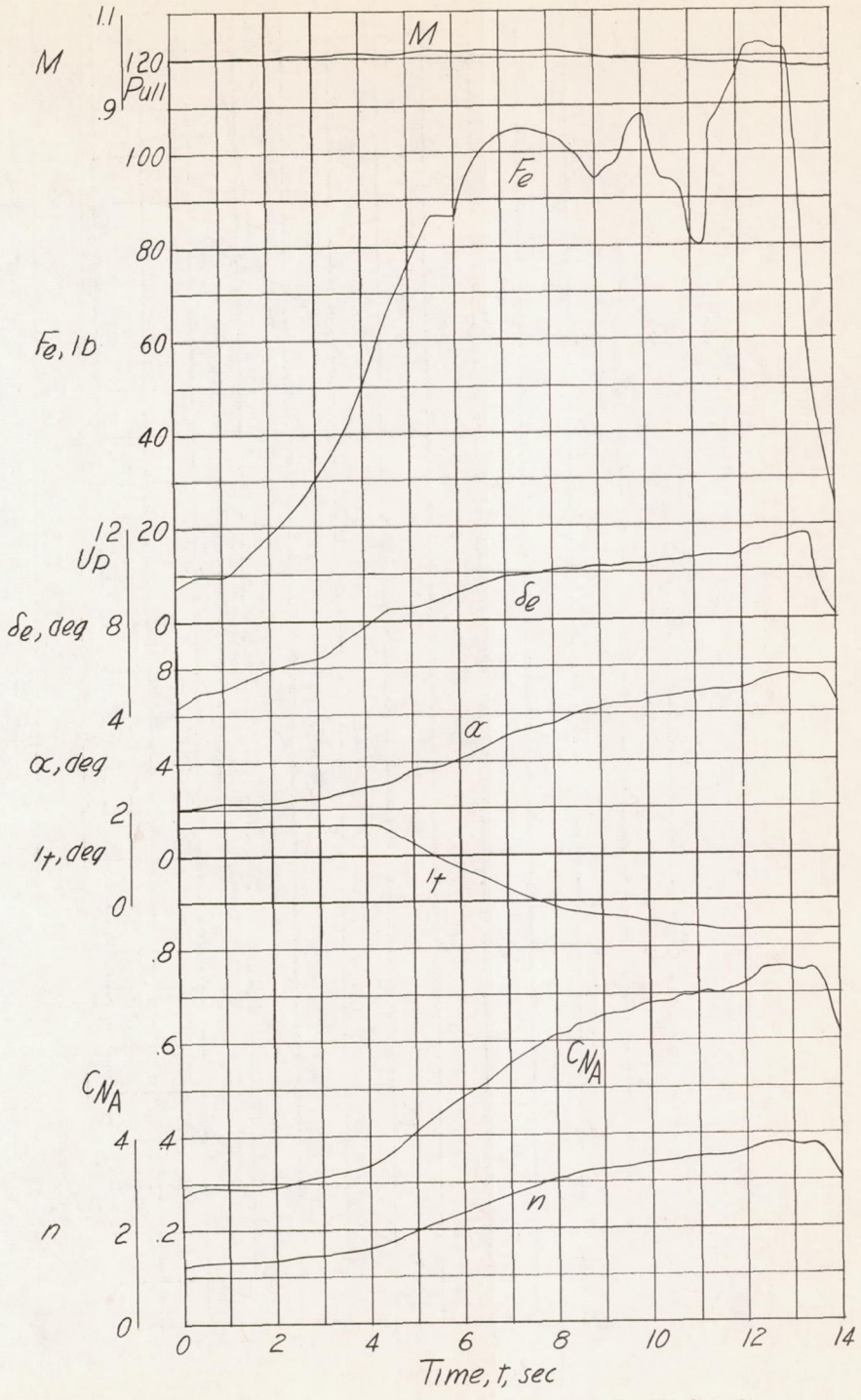

(k) $h_p \approx 34{,}000$ feet; center of gravity at 24.3 percent mean aerodynamic chord.

Figure 4.- Concluded.

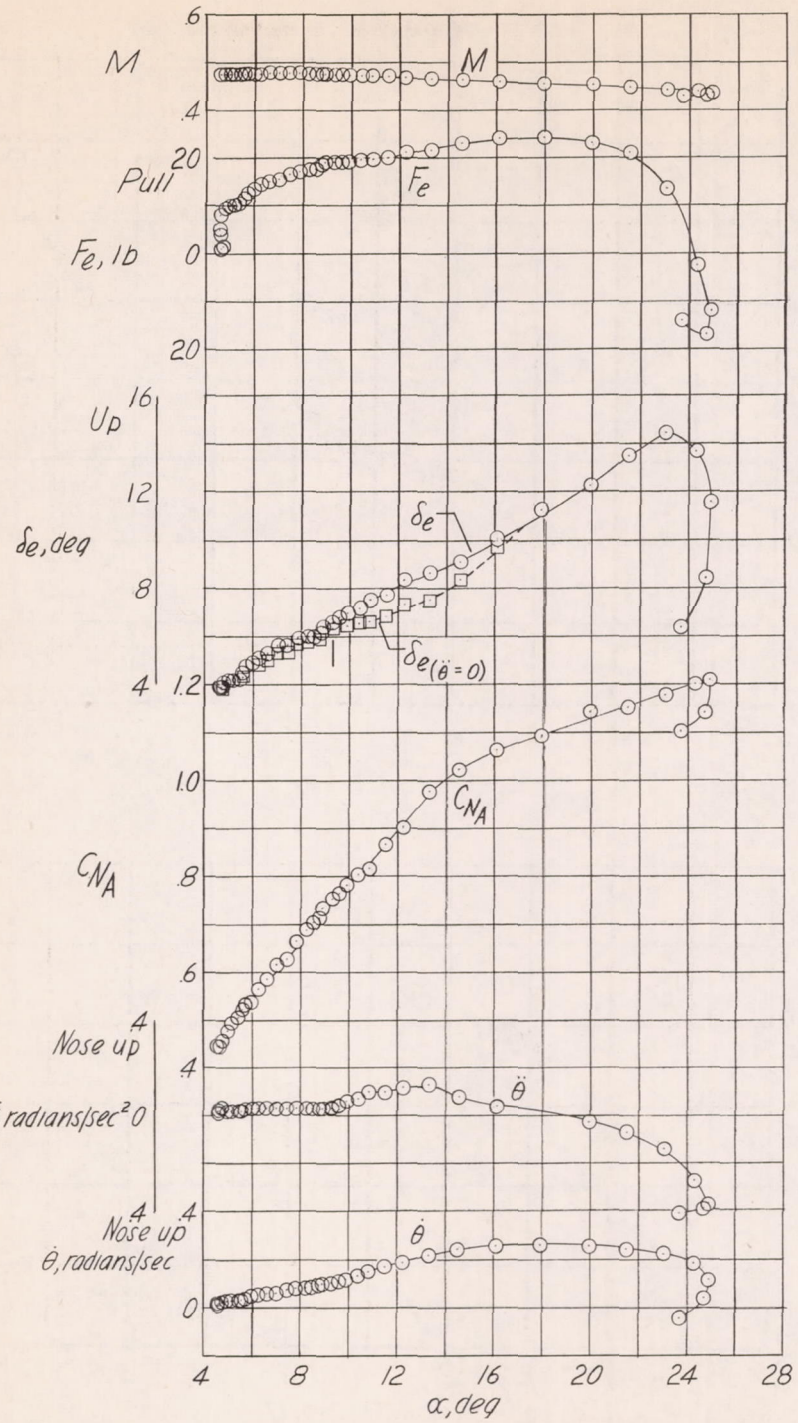

(a) $h_p \approx 20{,}100$ feet; $i_t = 1.6^\circ$; center of gravity at 22.8 percent mean aerodynamic chord.

Figure 5.- Static longitudinal stability characteristics of the Douglas D-558-II research airplane, equipped with wing chord-extensions, in turning flight.

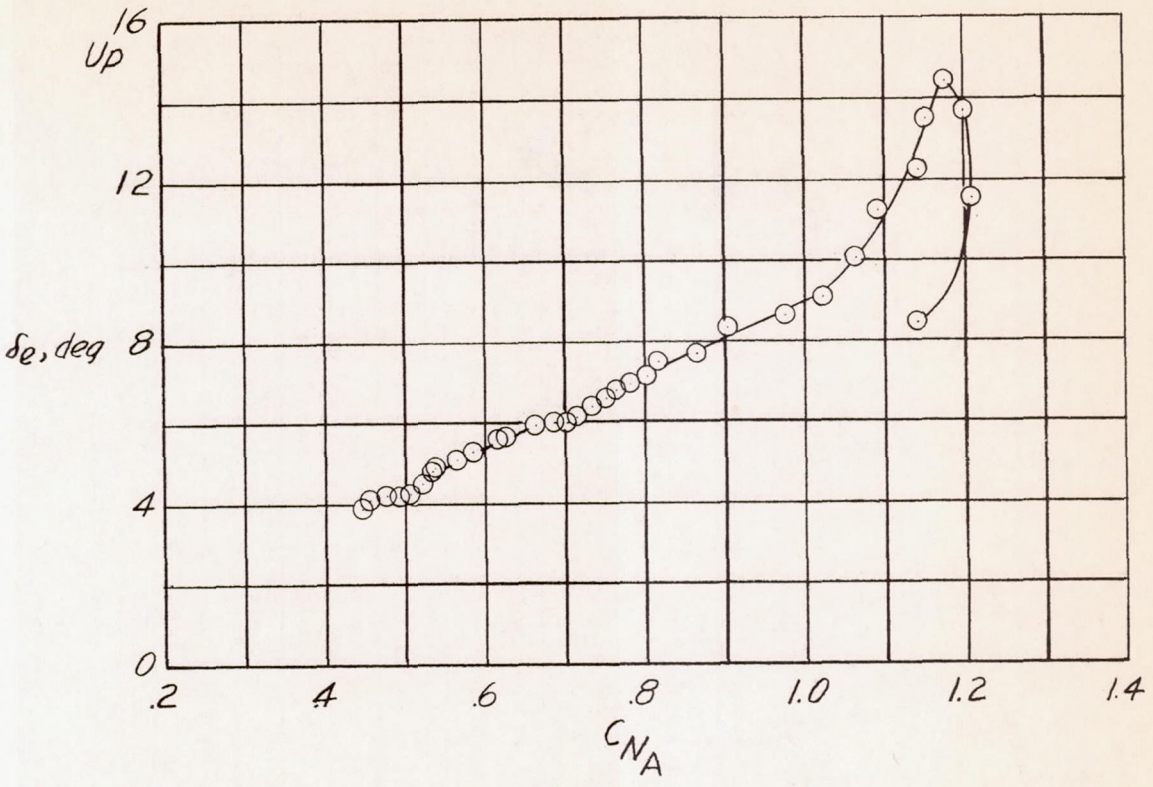

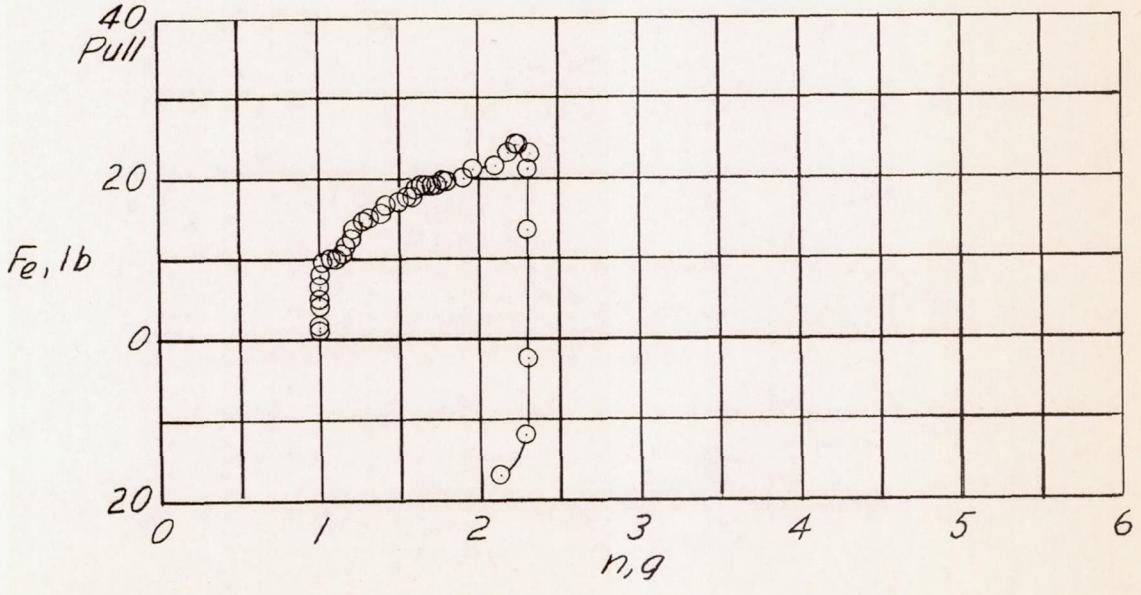

(a) Concluded.

Figure 5.- Continued.

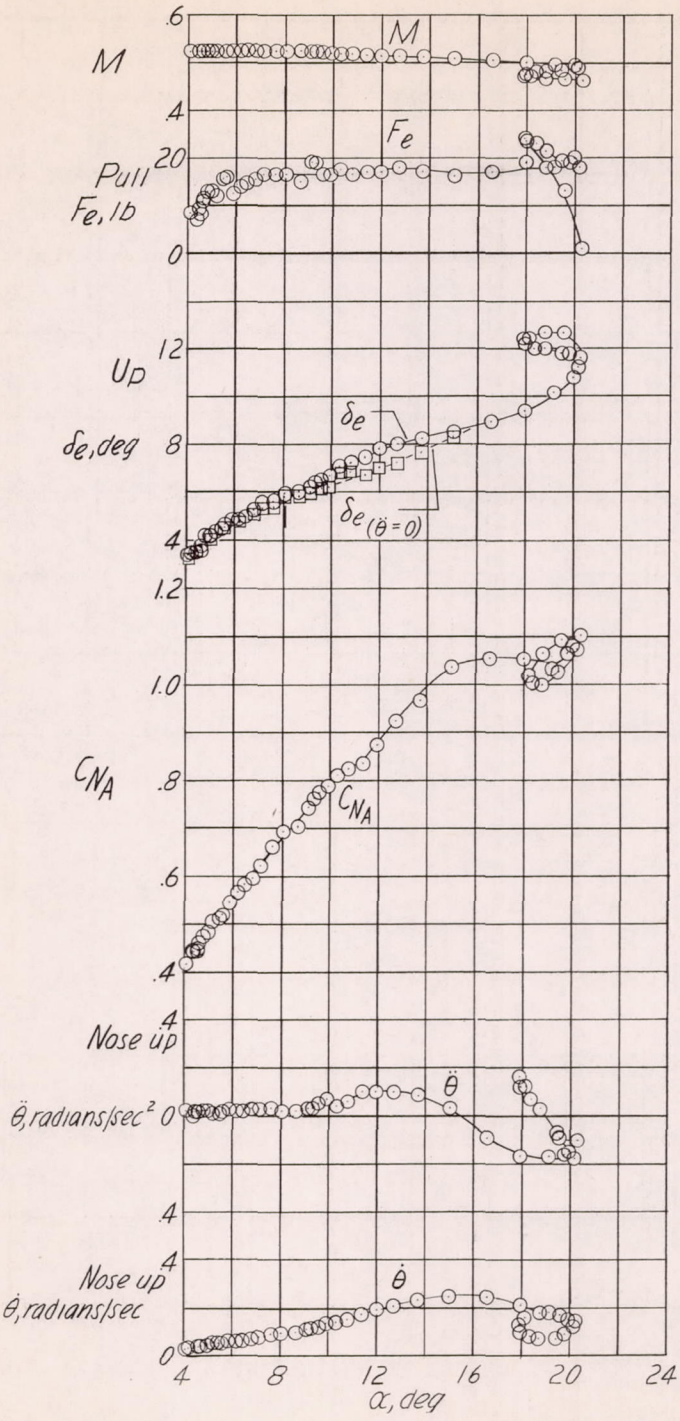

(b) $h_p \approx 21{,}600$ feet; $i_t = 1.6^\circ$; center of gravity at 22.8 percent mean aerodynamic chord.

Figure 5.- Continued.

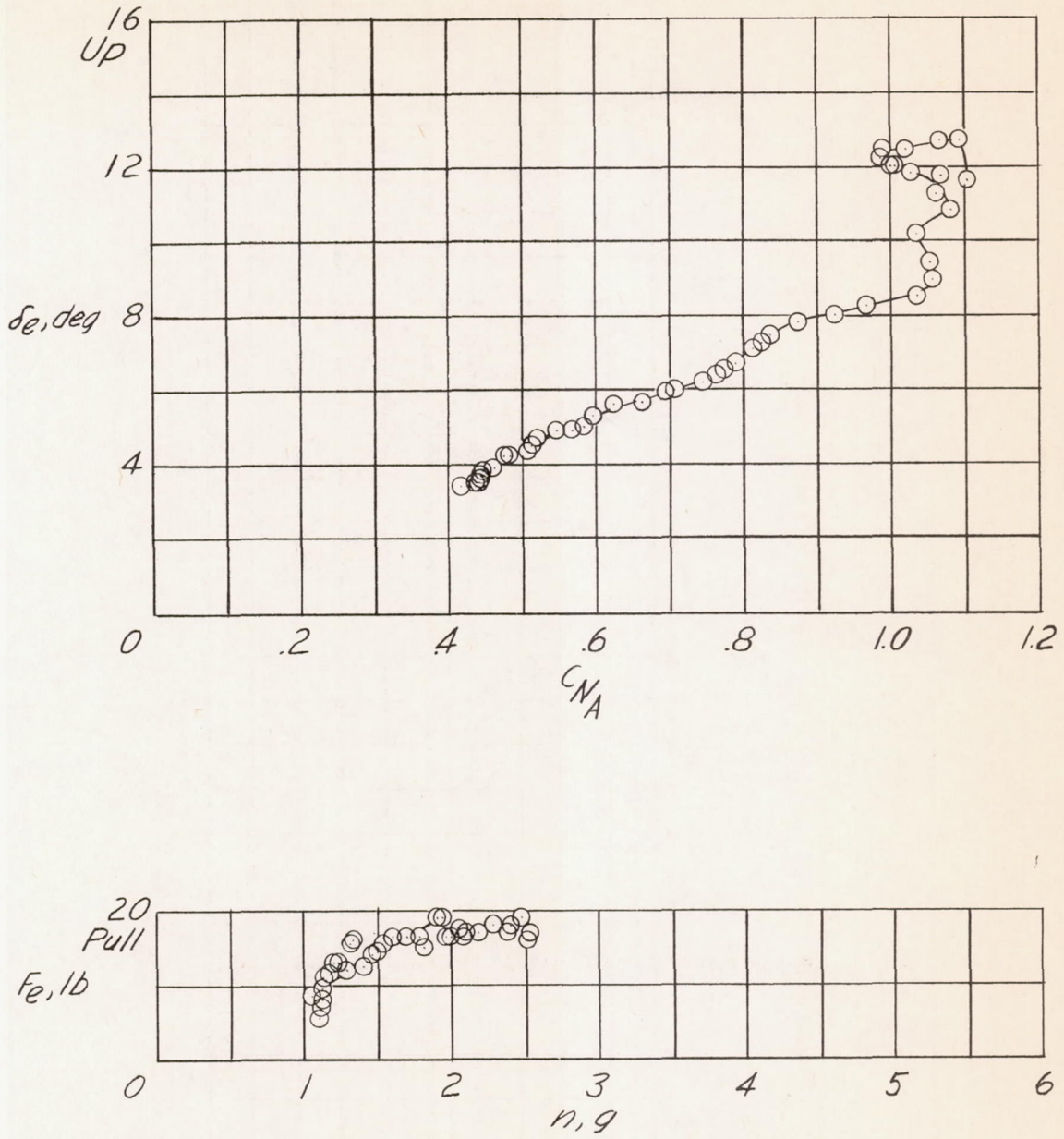

(b) Concluded.

Figure 5.- Continued.

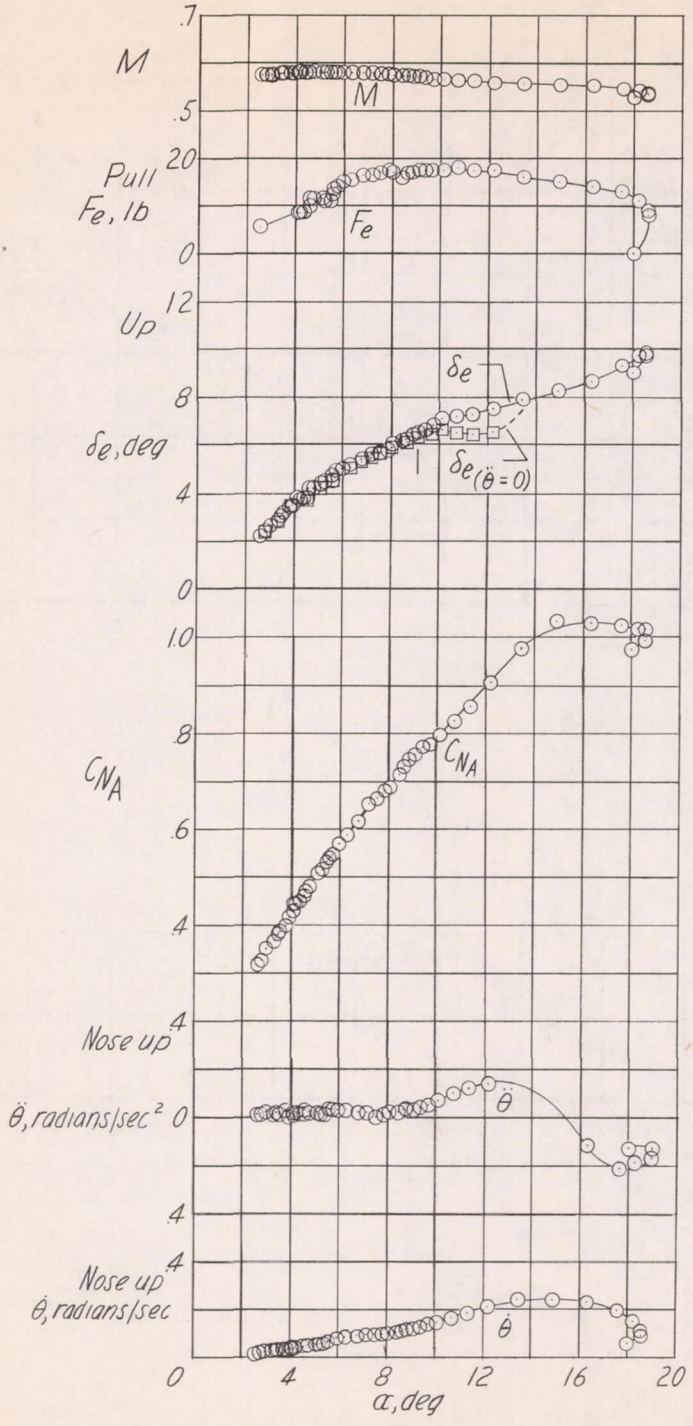

(c) $h_p \approx 22{,}800$ feet; $i_t = 1.6^\circ$; center of gravity at 22.7 percent mean aerodynamic chord.

Figure 5.- Continued.

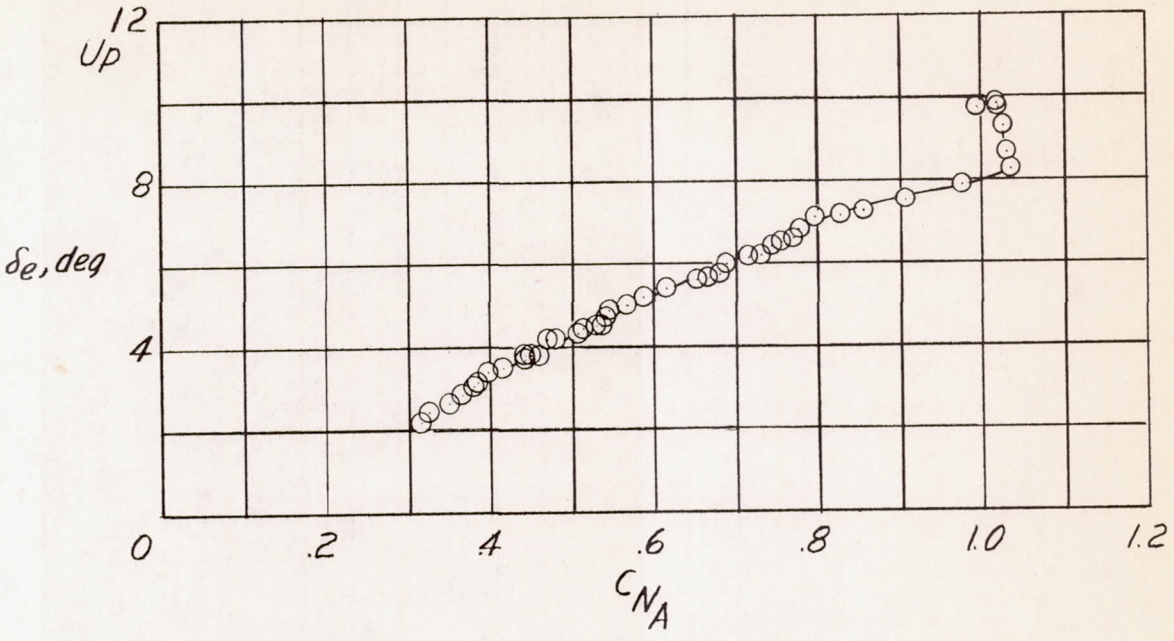

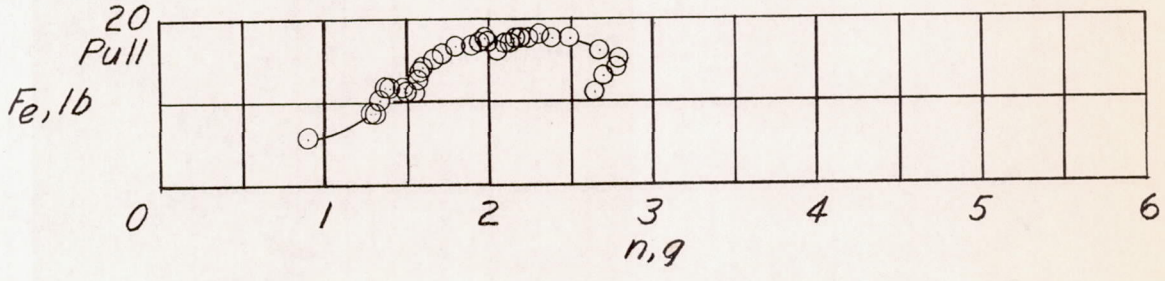

(c) Concluded.

Figure 5.- Continued.

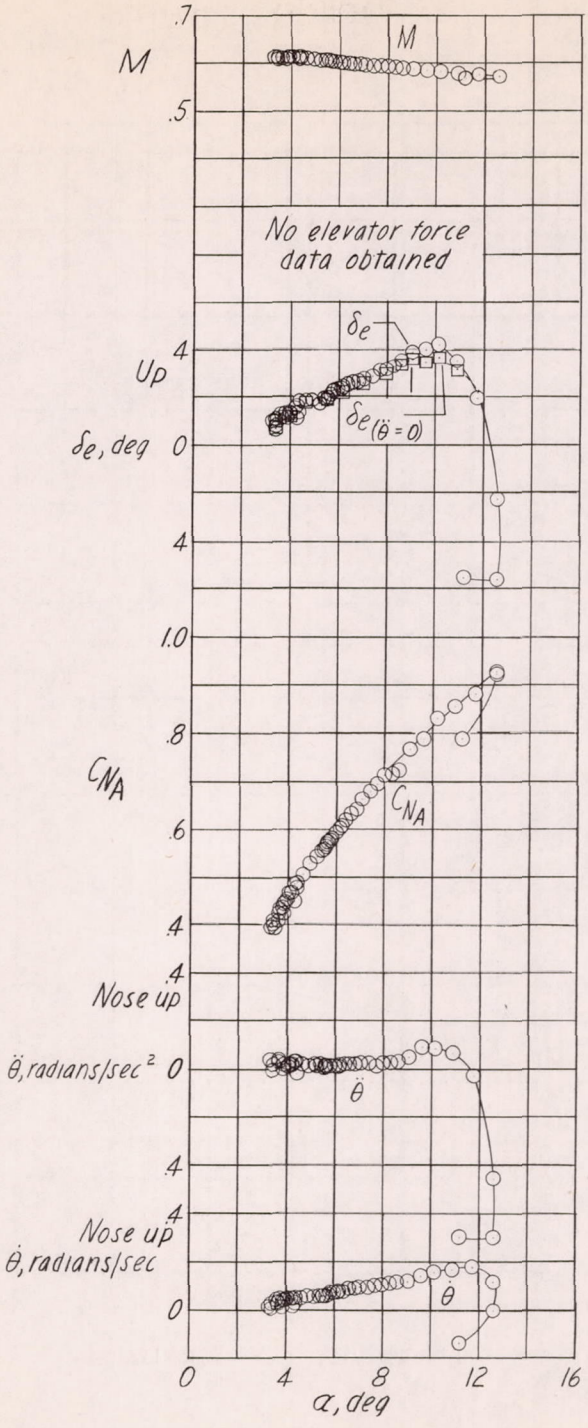

(d) $h_p \approx 24{,}100$ feet; $i_t = 1.3^\circ$; center of gravity at 28.0 percent mean aerodynamic chord.

Figure 5.- Continued.

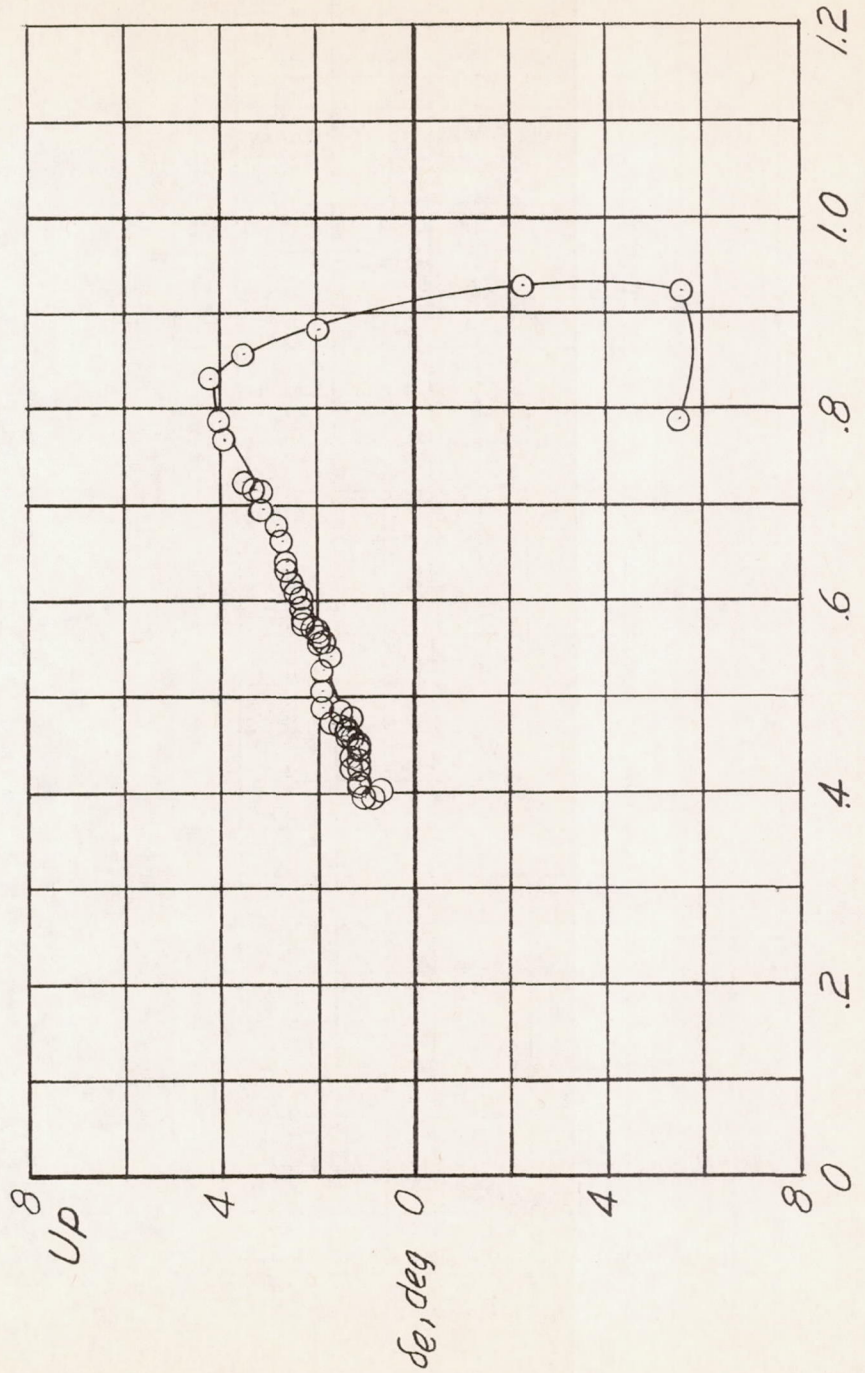

(d) Concluded.

Figure 5.- Continued.

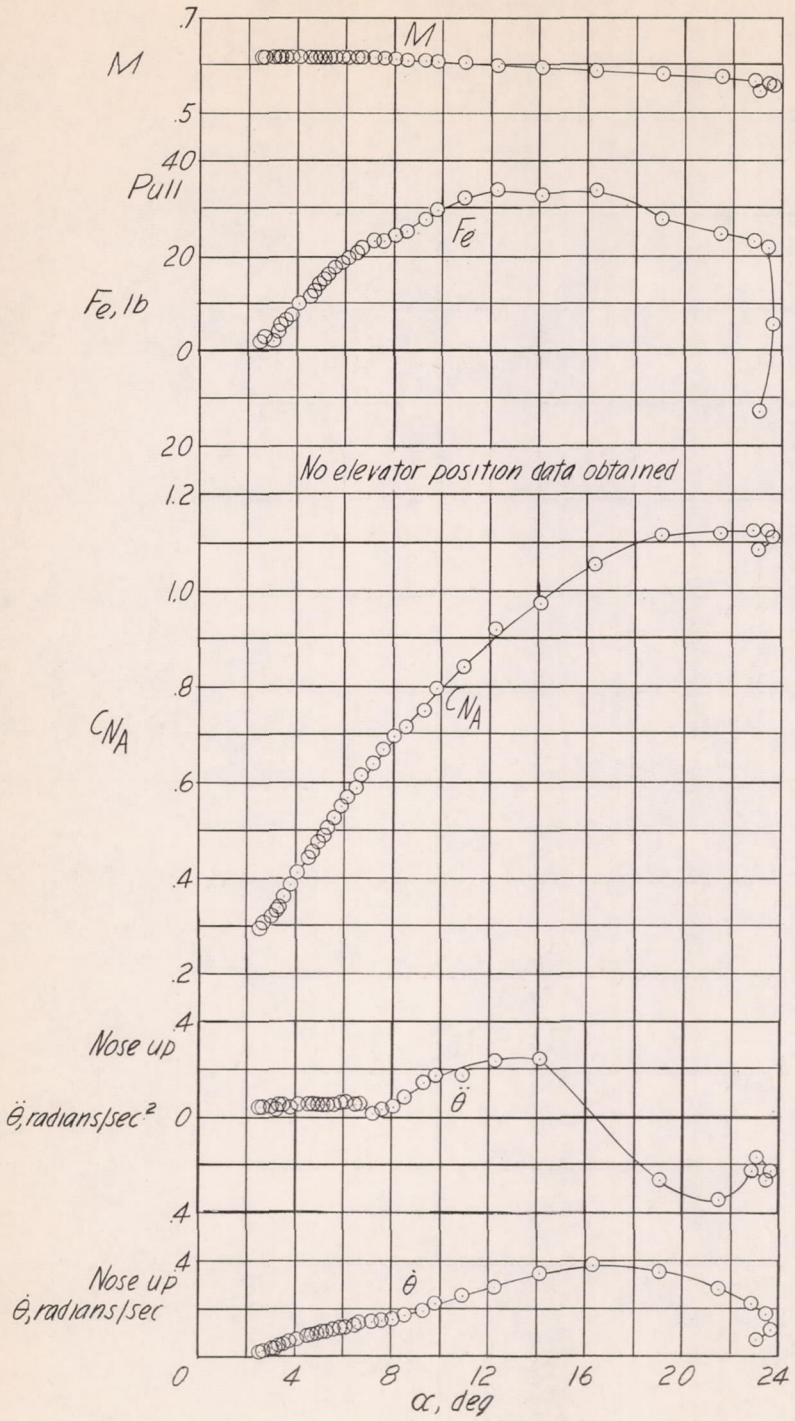

(e) $h_p \approx 21{,}500$ feet; $i_t = 1.7°$; center of gravity at 24.1 percent mean aerodynamic chord.

Figure 5.- Continued.

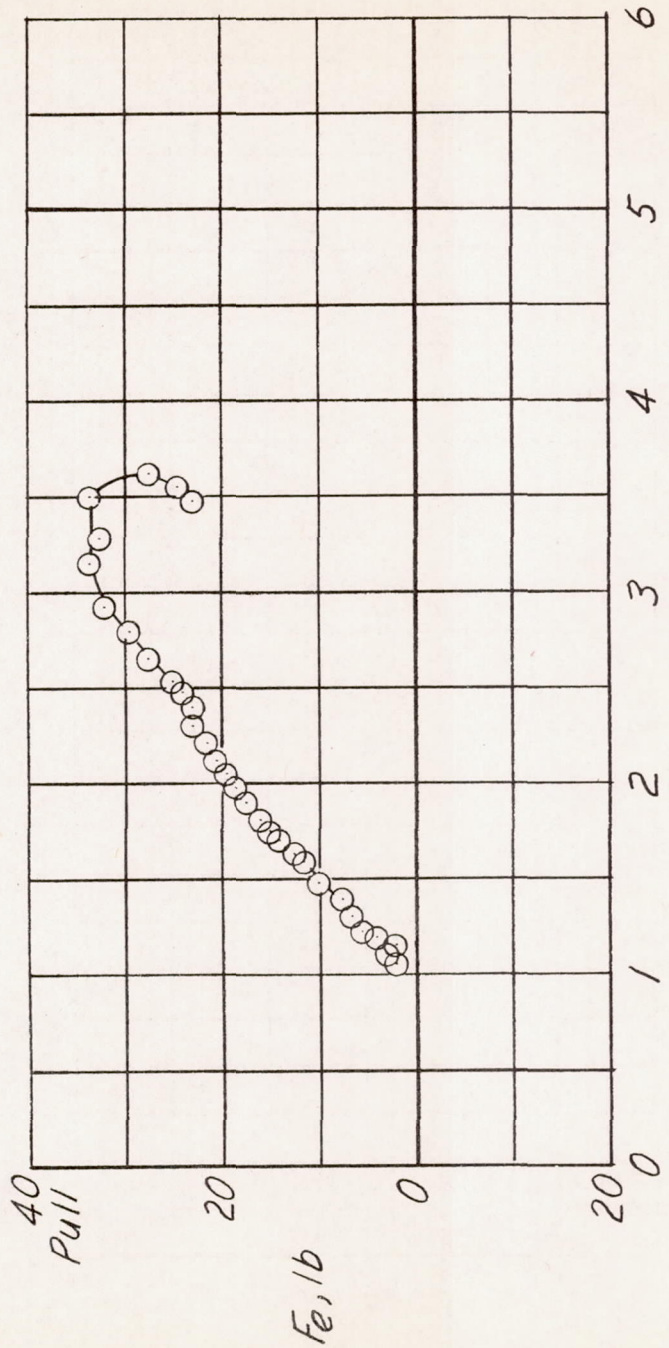

(e) Concluded.

Figure 5.- Continued.

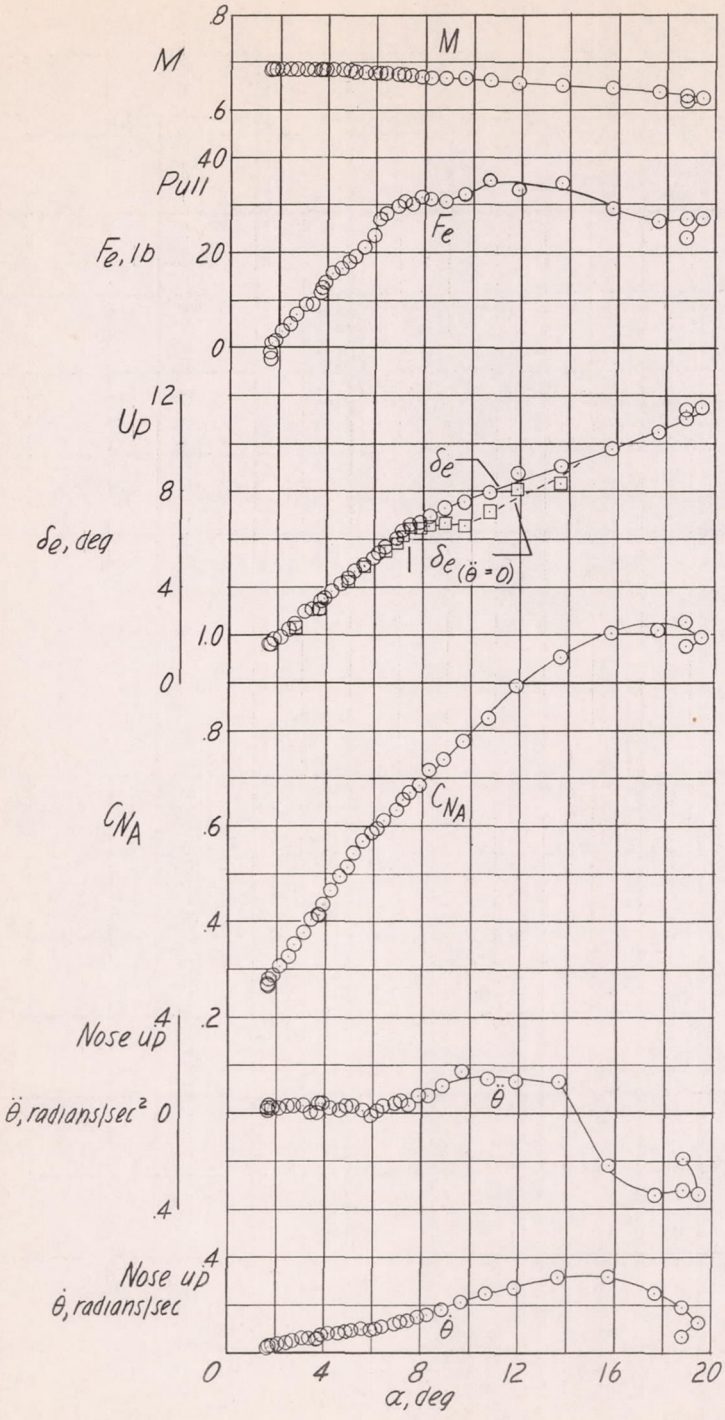

(f) $h_p \approx 23{,}500$ feet; $i_t = 1.7^\circ$; center of gravity at 24.1 percent mean aerodynamic chord.

Figure 5.- Continued.

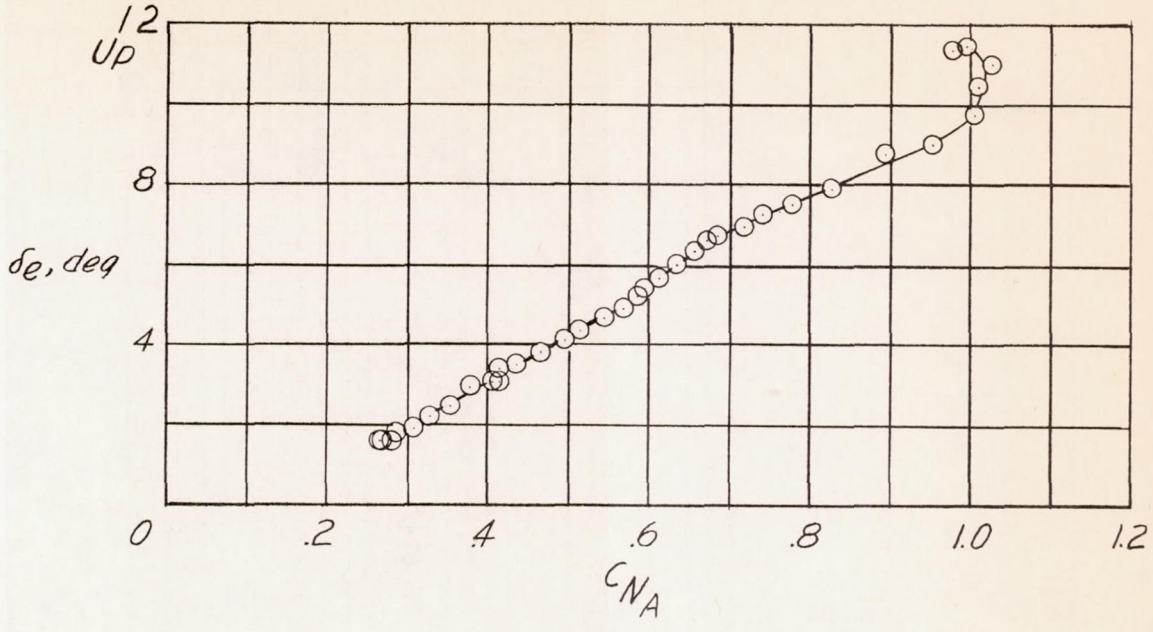

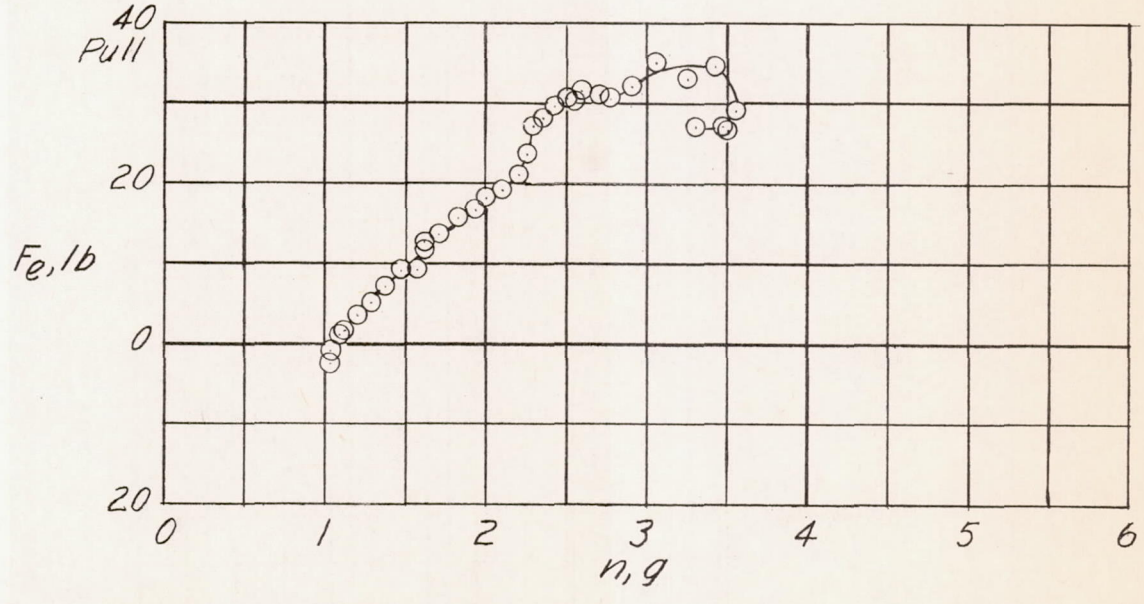

(f) Concluded.

Figure 5.- Continued.

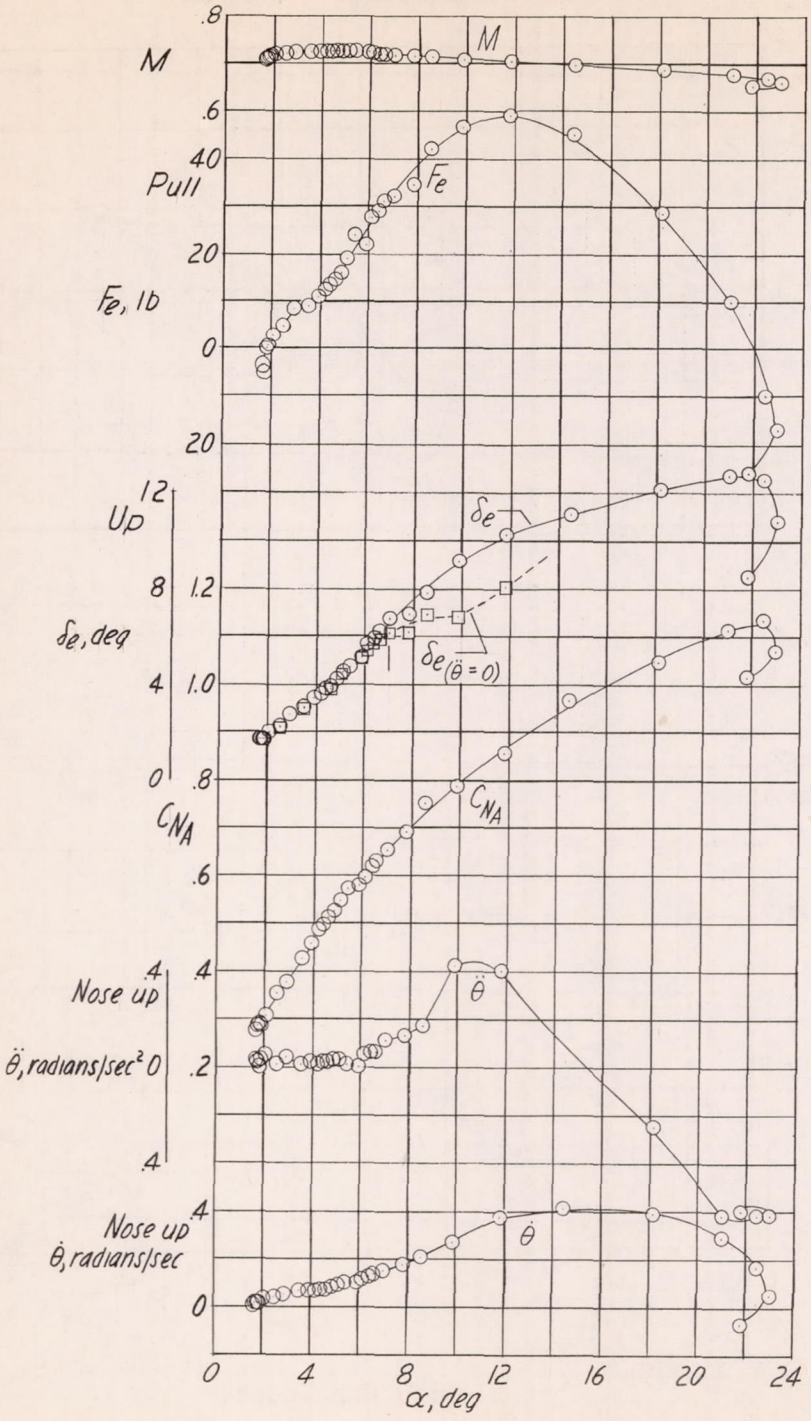

(g) $h_p \approx 25{,}300$ feet; $i_t = 1.6^\circ$; center of gravity at 22.6 percent mean aerodynamic chord.

Figure 5.- Continued.

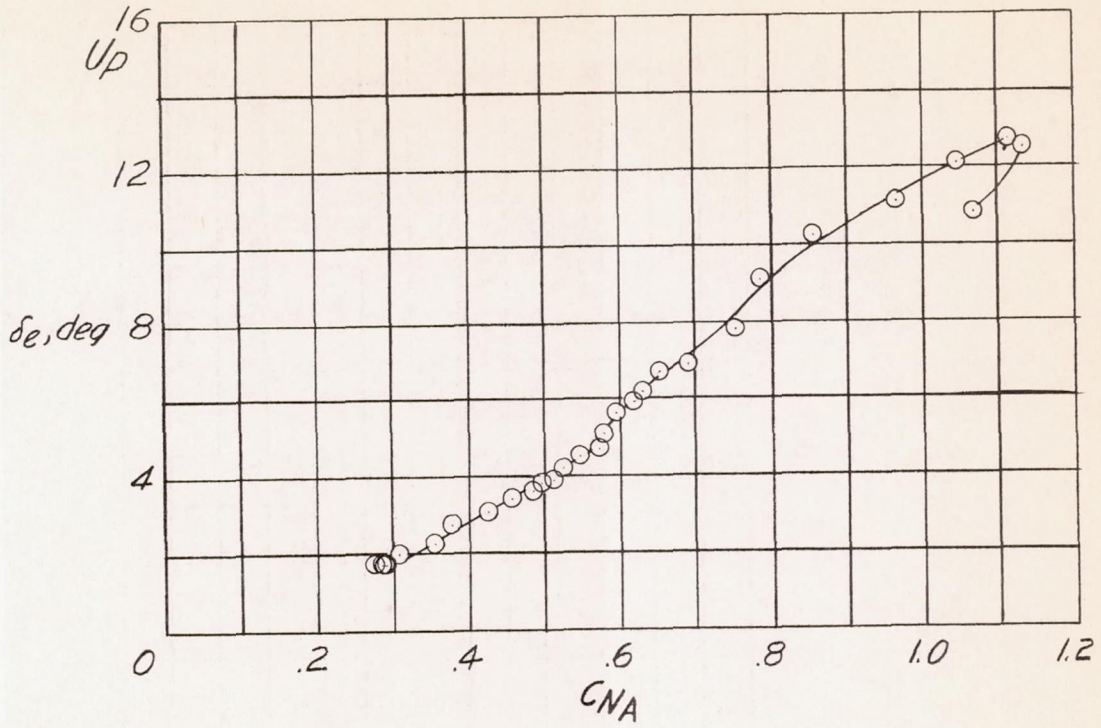

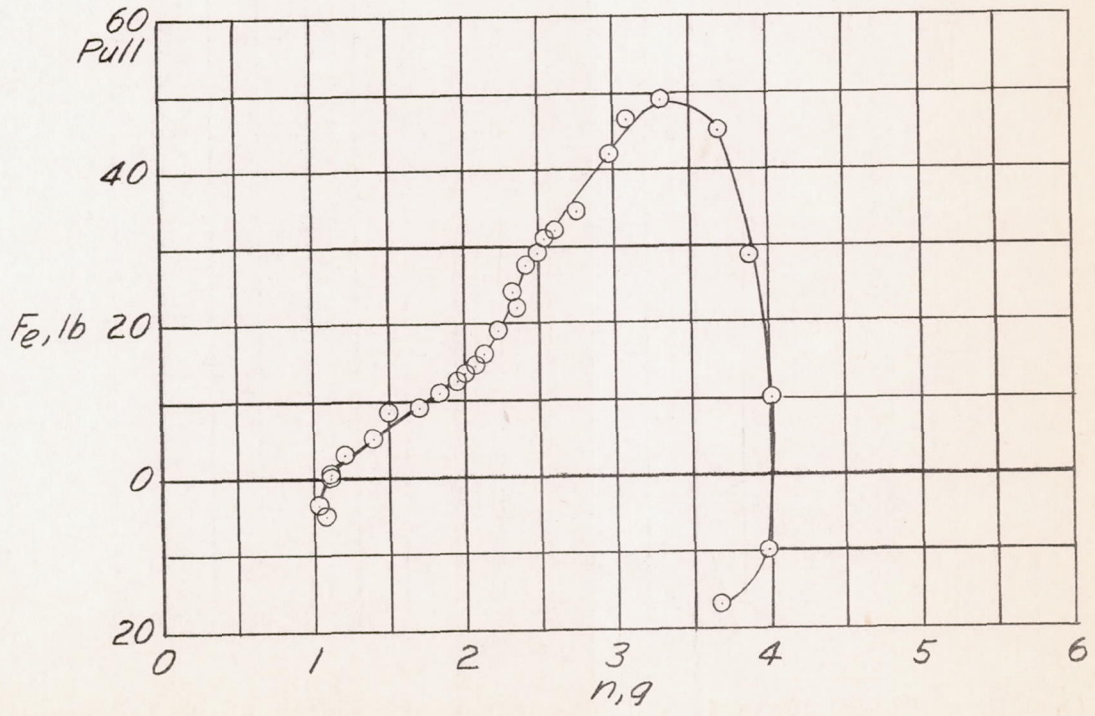

(g) Concluded.

Figure 5.- Continued.

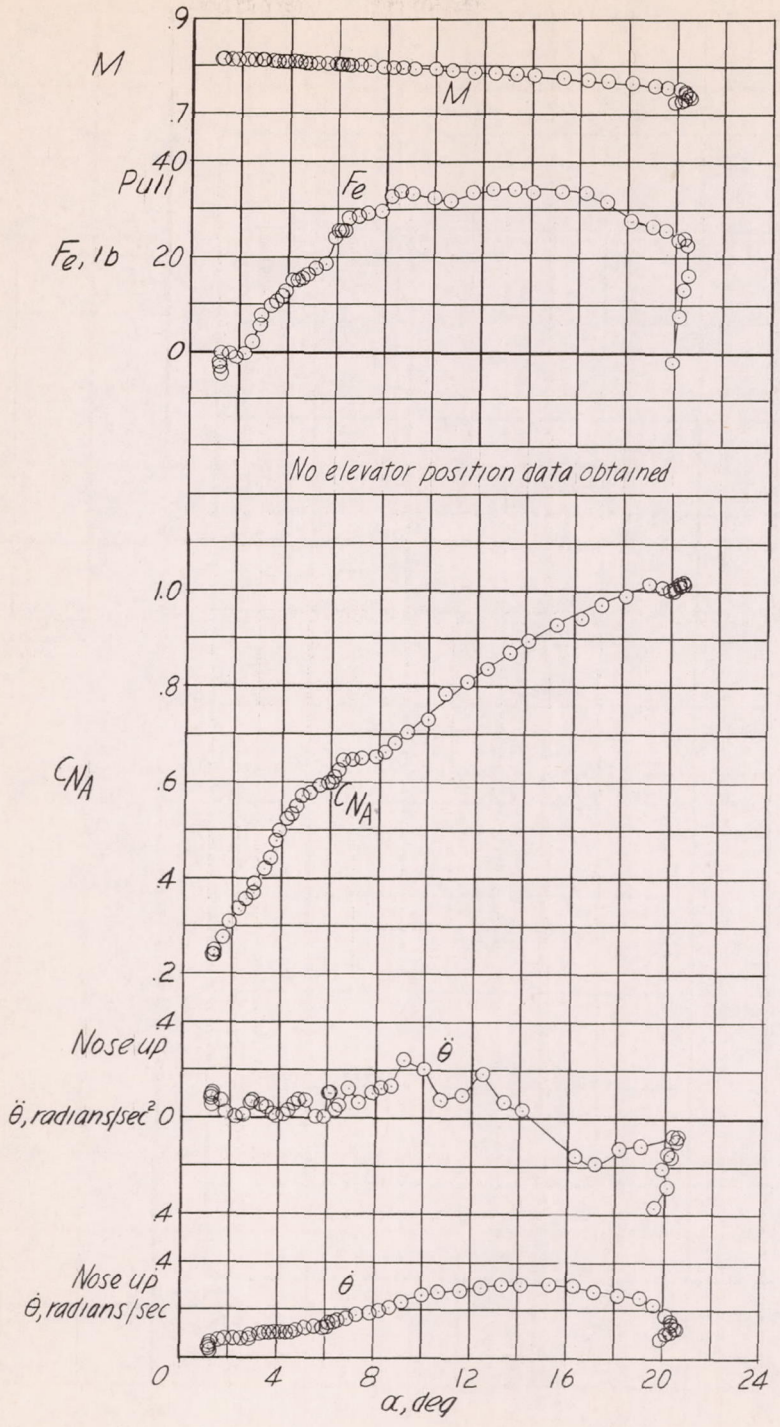

(h) $h_p \approx 28{,}900$ feet; $i_t = 1.7°$; center of gravity at 24.1 percent mean aerodynamic chord.

Figure 5.- Continued.

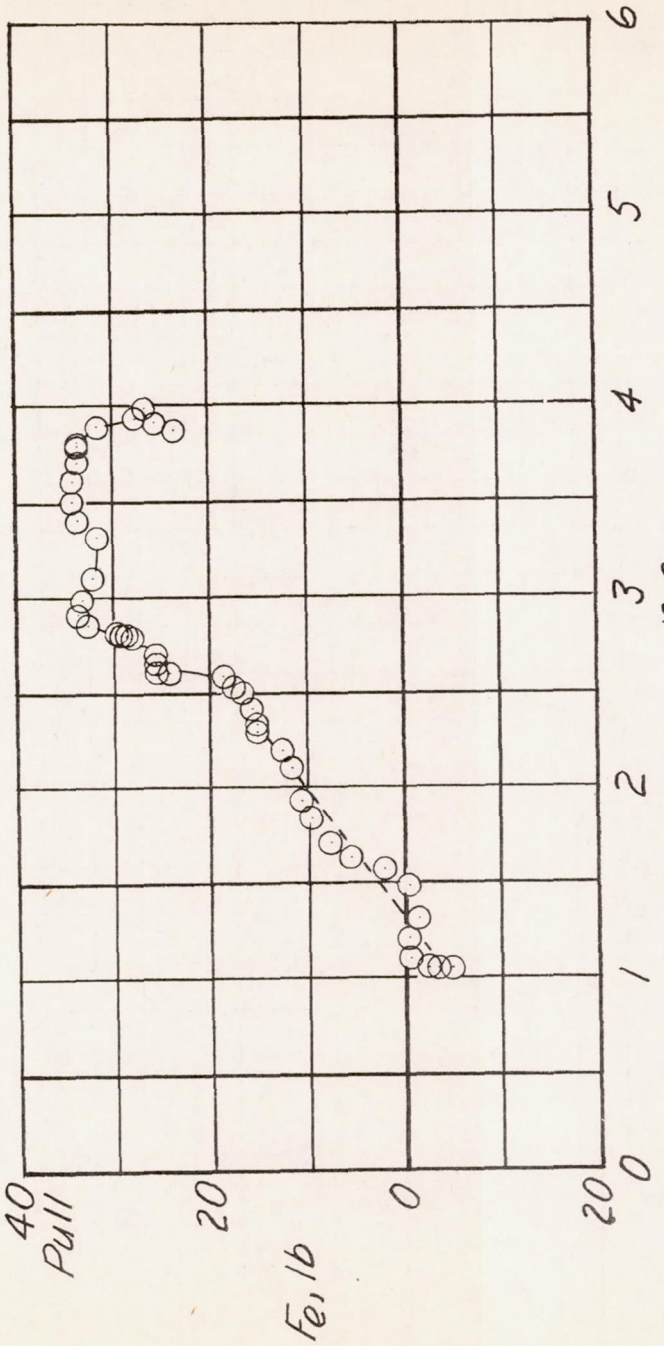

(h) Concluded.

Figure 5.- Continued.

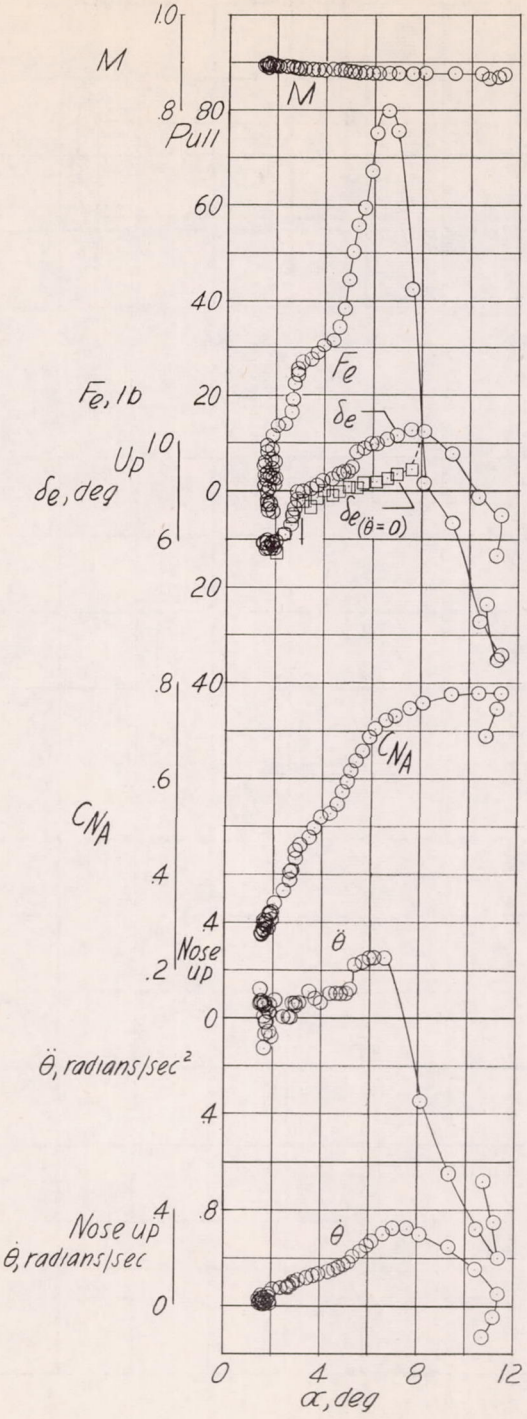

(i) $h_p \approx 30{,}800$ feet; $i_t = 1.7^\circ$; center of gravity at 24.7 percent mean aerodynamic chord.

Figure 5.- Continued.

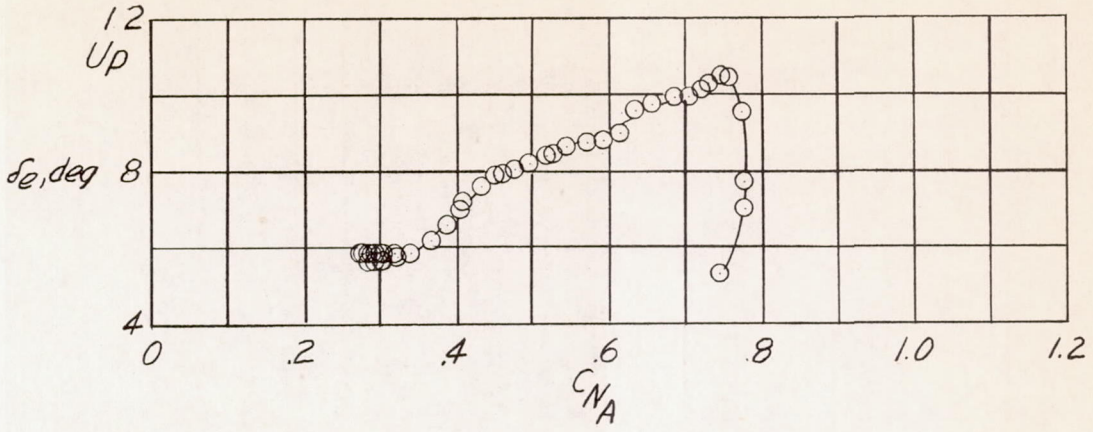

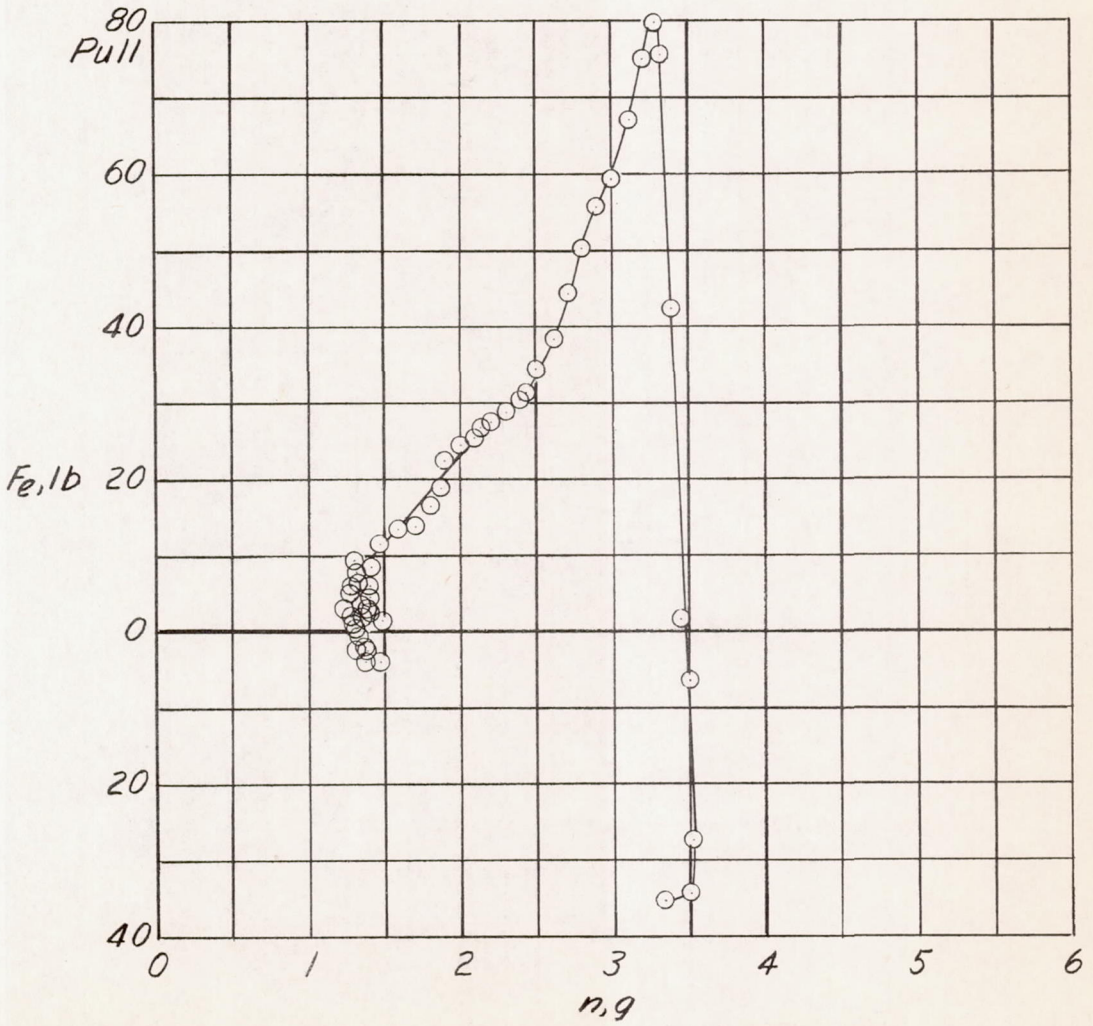

(i) Concluded.

Figure 5.- Continued.

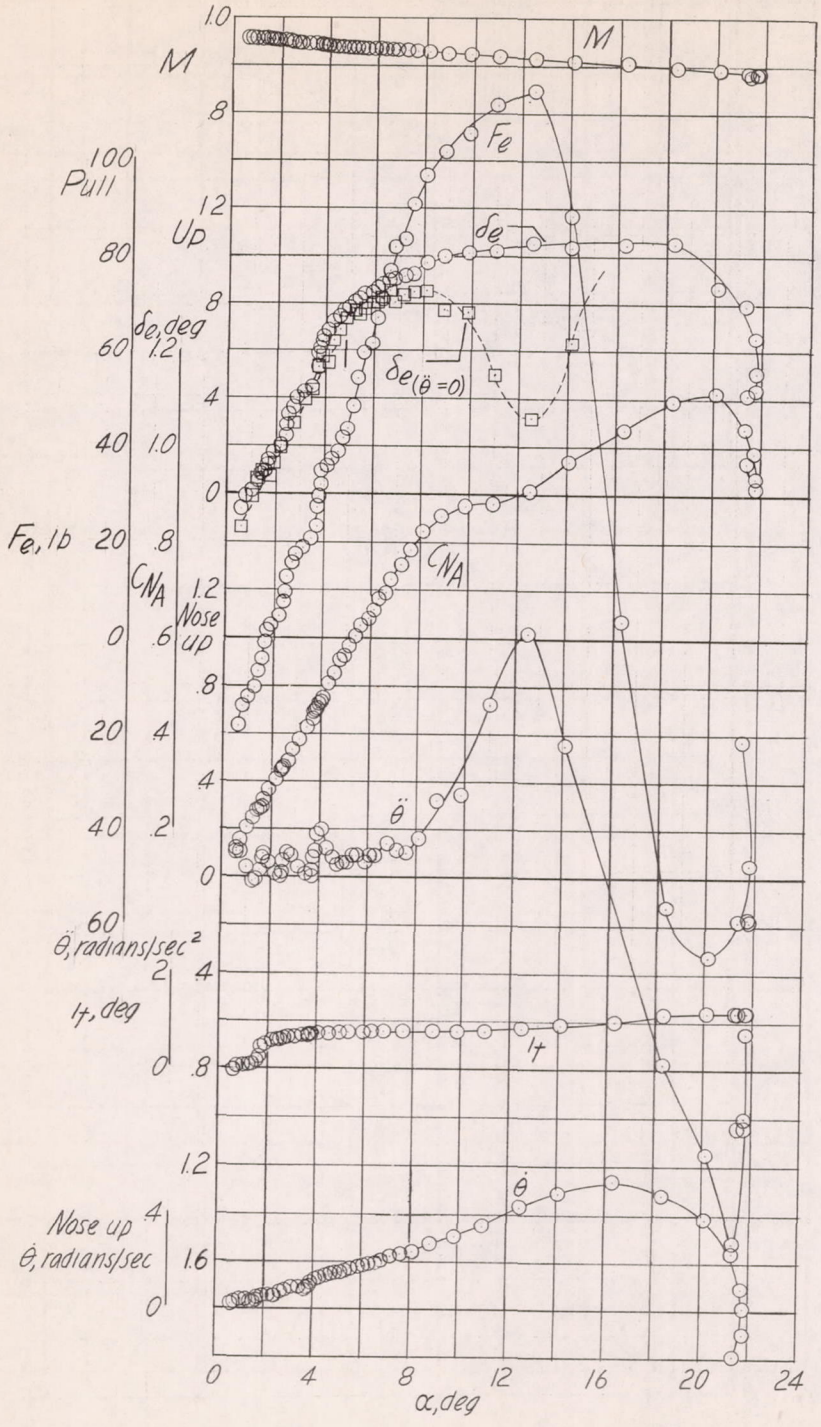

(j) $h_p \approx 32{,}000$ feet; center of gravity at 24.6 percent mean aerodynamic chord.

Figure 5.- Continued.

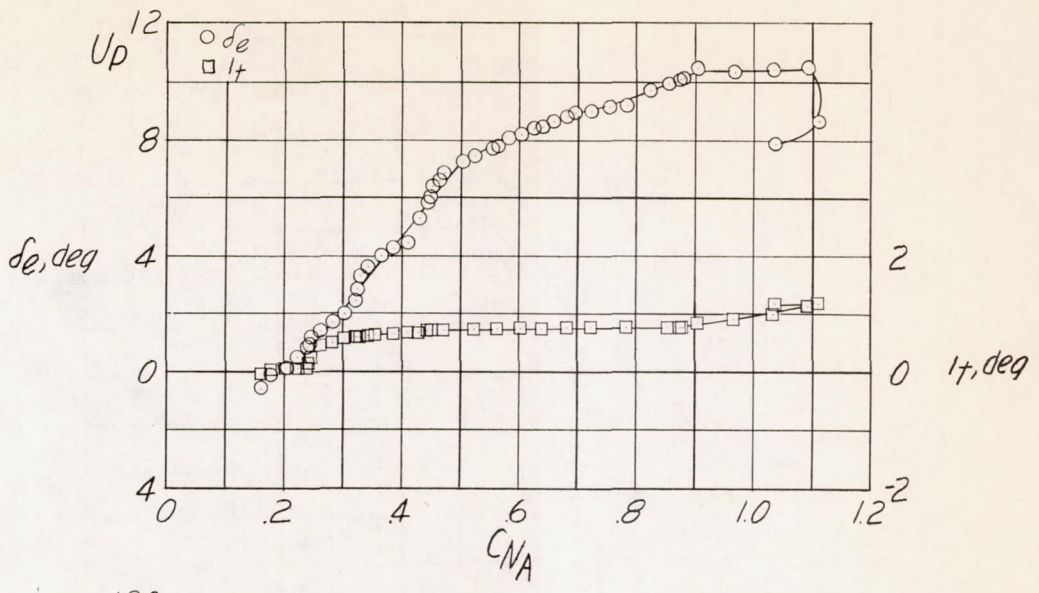

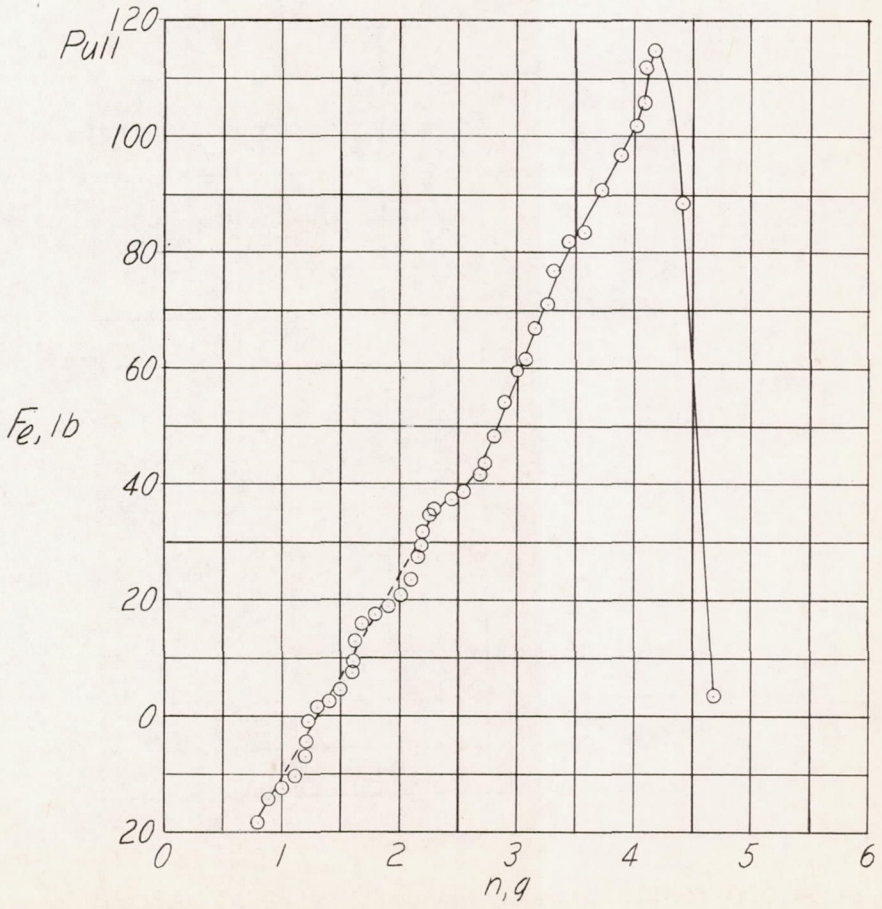

(j) Concluded.

Figure 5.- Continued.

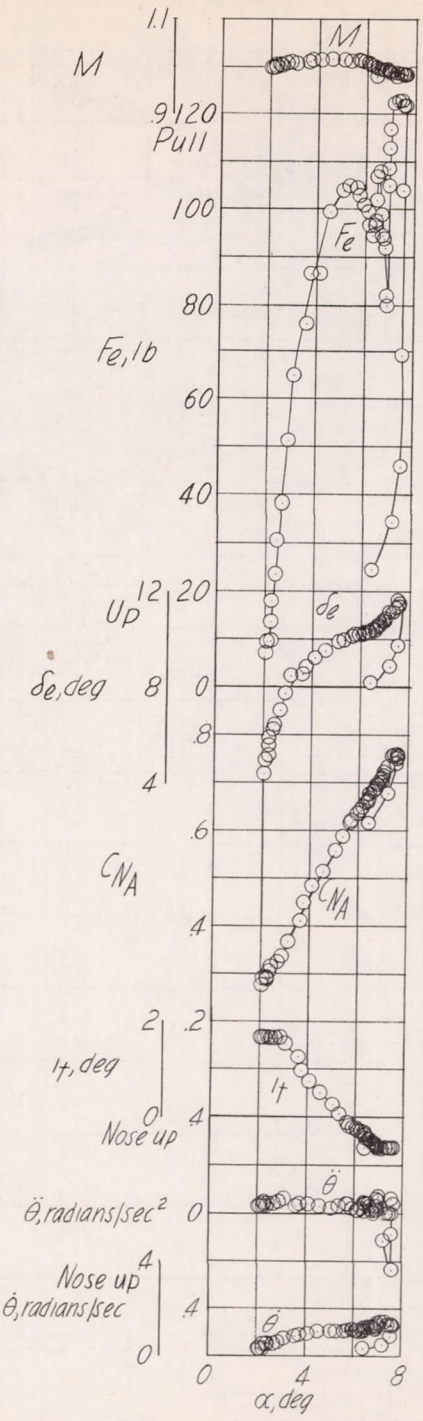

(k) $h_p \approx 34{,}000$ feet; center of gravity at 24.3 percent mean aerodynamic chord.

Figure 5.- Continued.

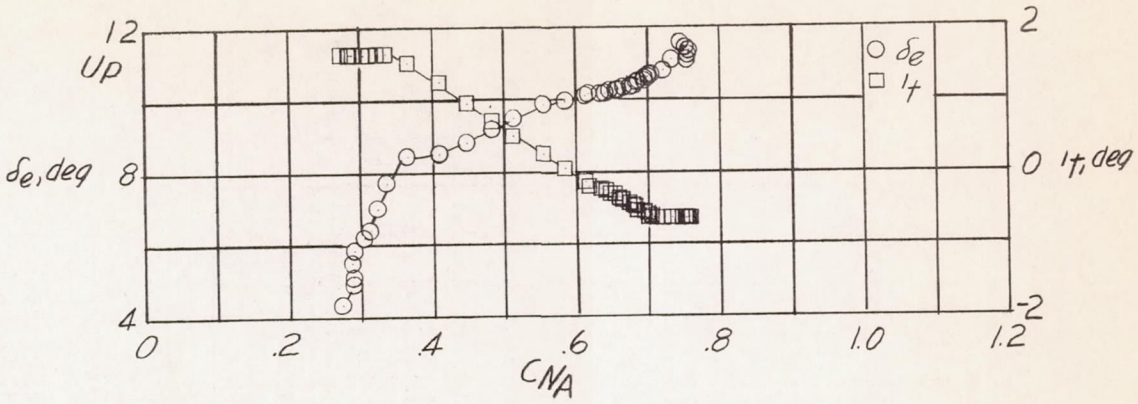

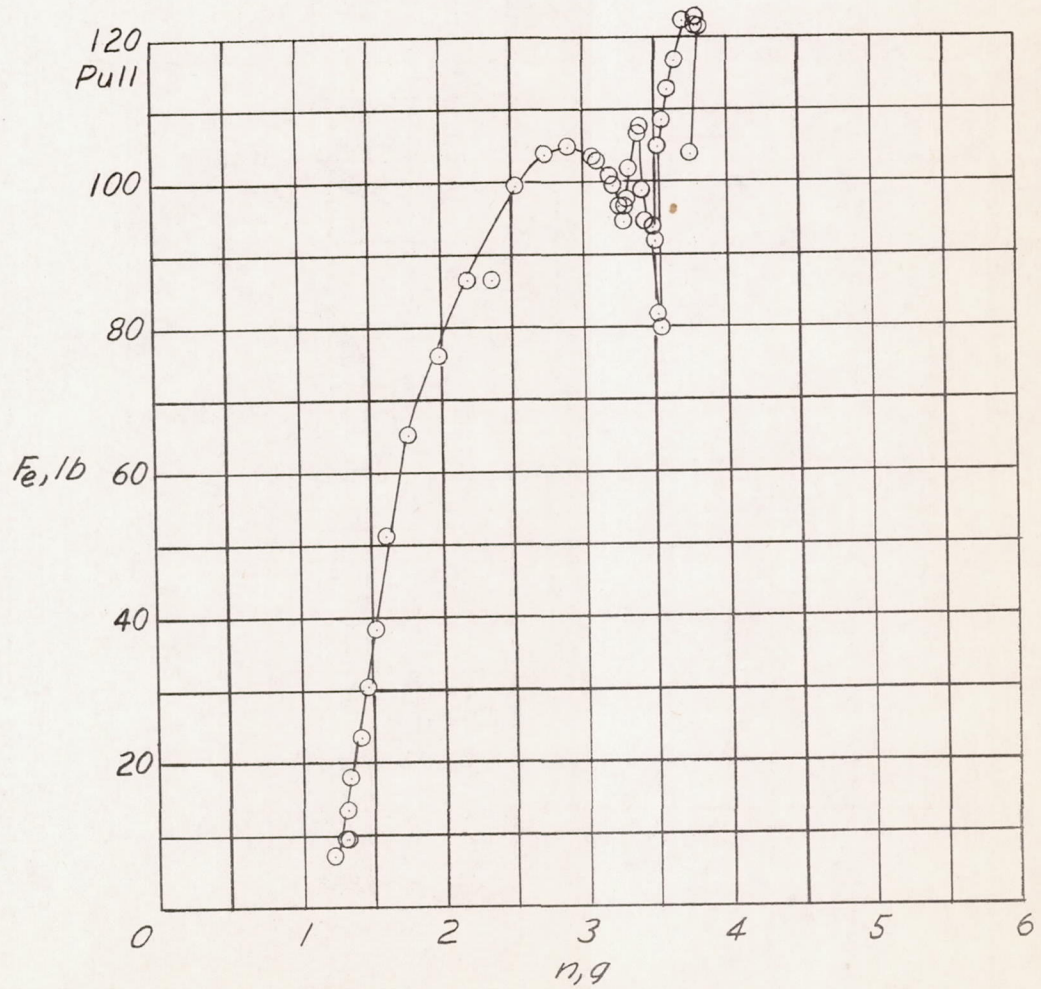

(k) Concluded.

Figure 5.- Concluded.

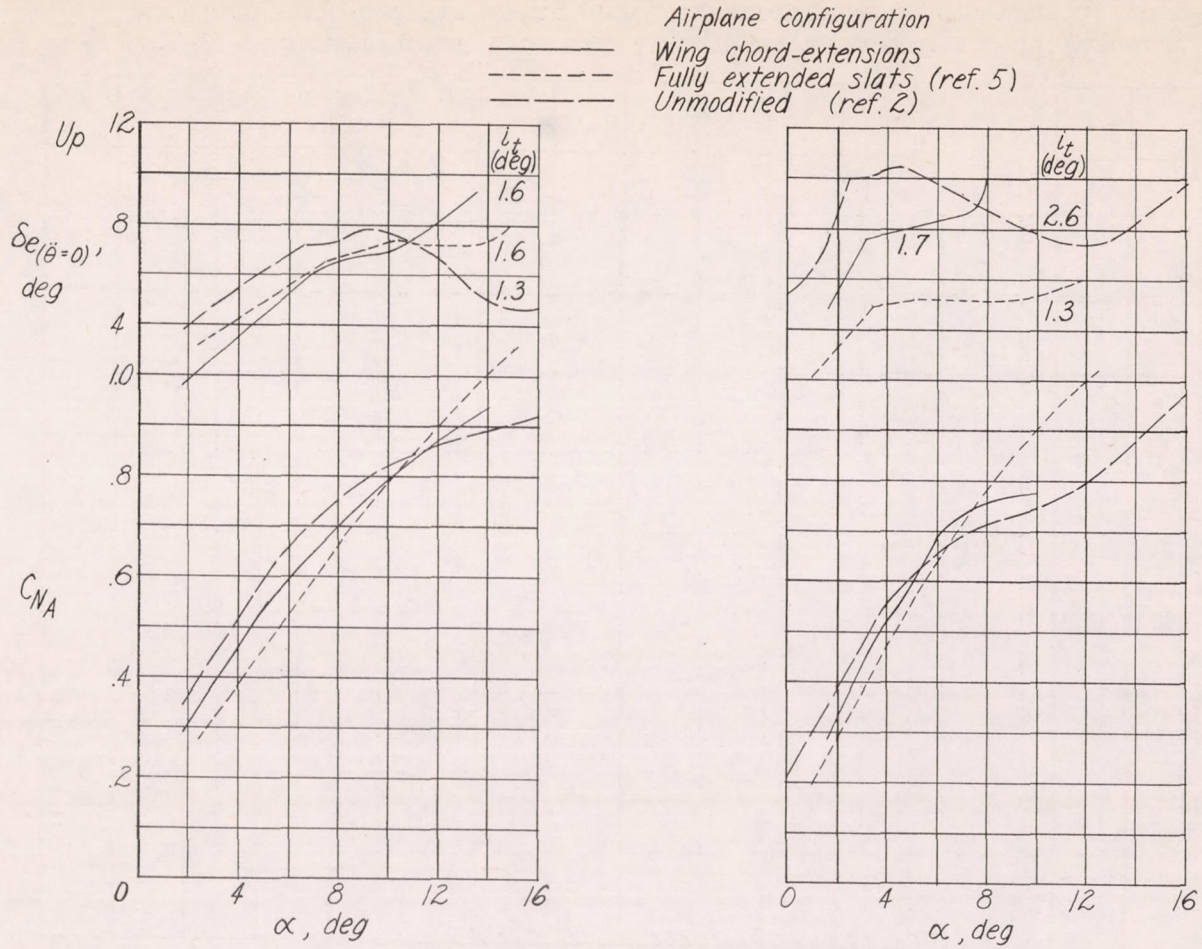

(a) M ≈ 0.7.

(b) M ≈ 0.9.

Figure 6.- Effect of various modifications on the static longitudinal stability characteristics of the D-558-II research airplane in turning flight.

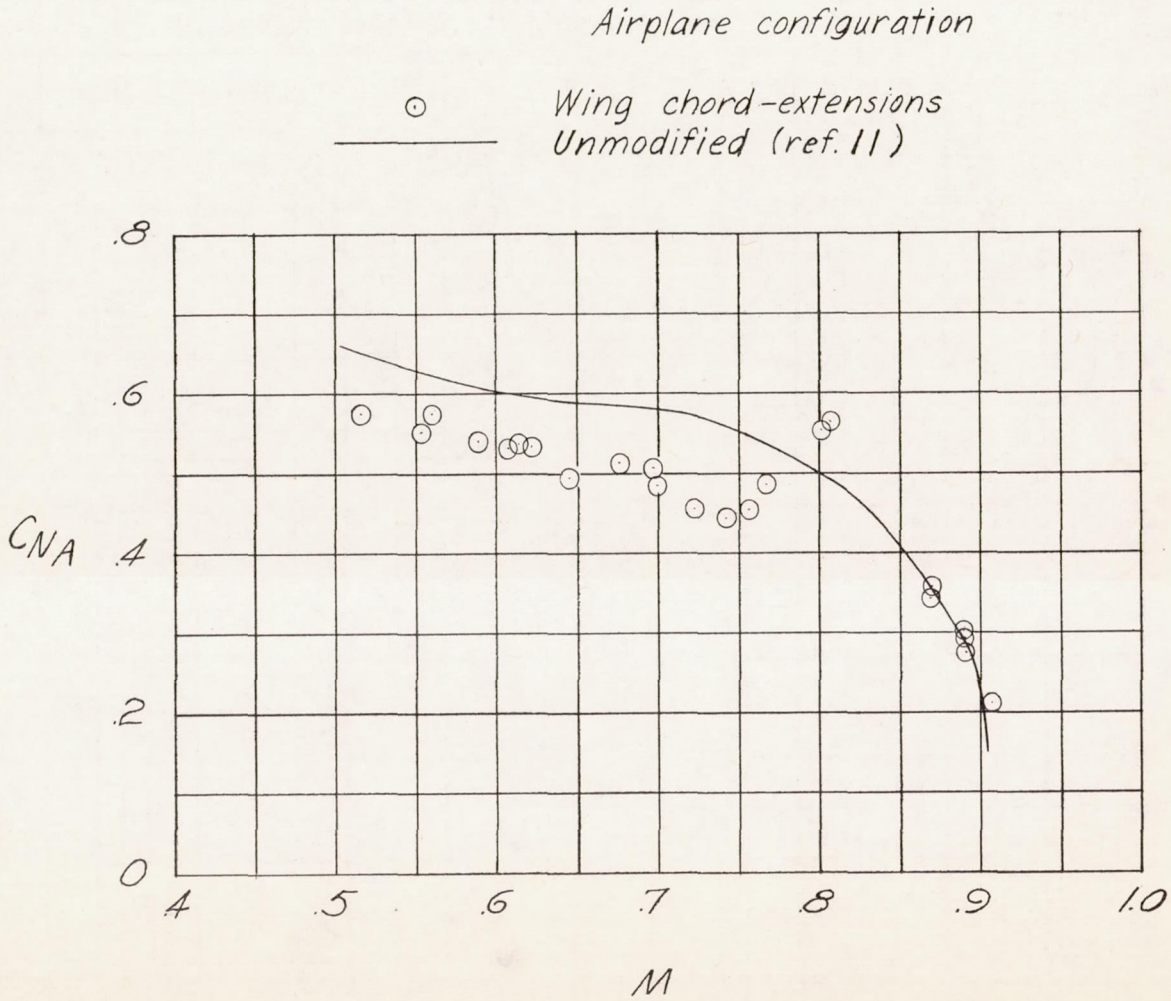

Figure 7.- Comparison of the buffet boundary of the D-558-II research airplane equipped with wing chord extensions with the unmodified configuration.

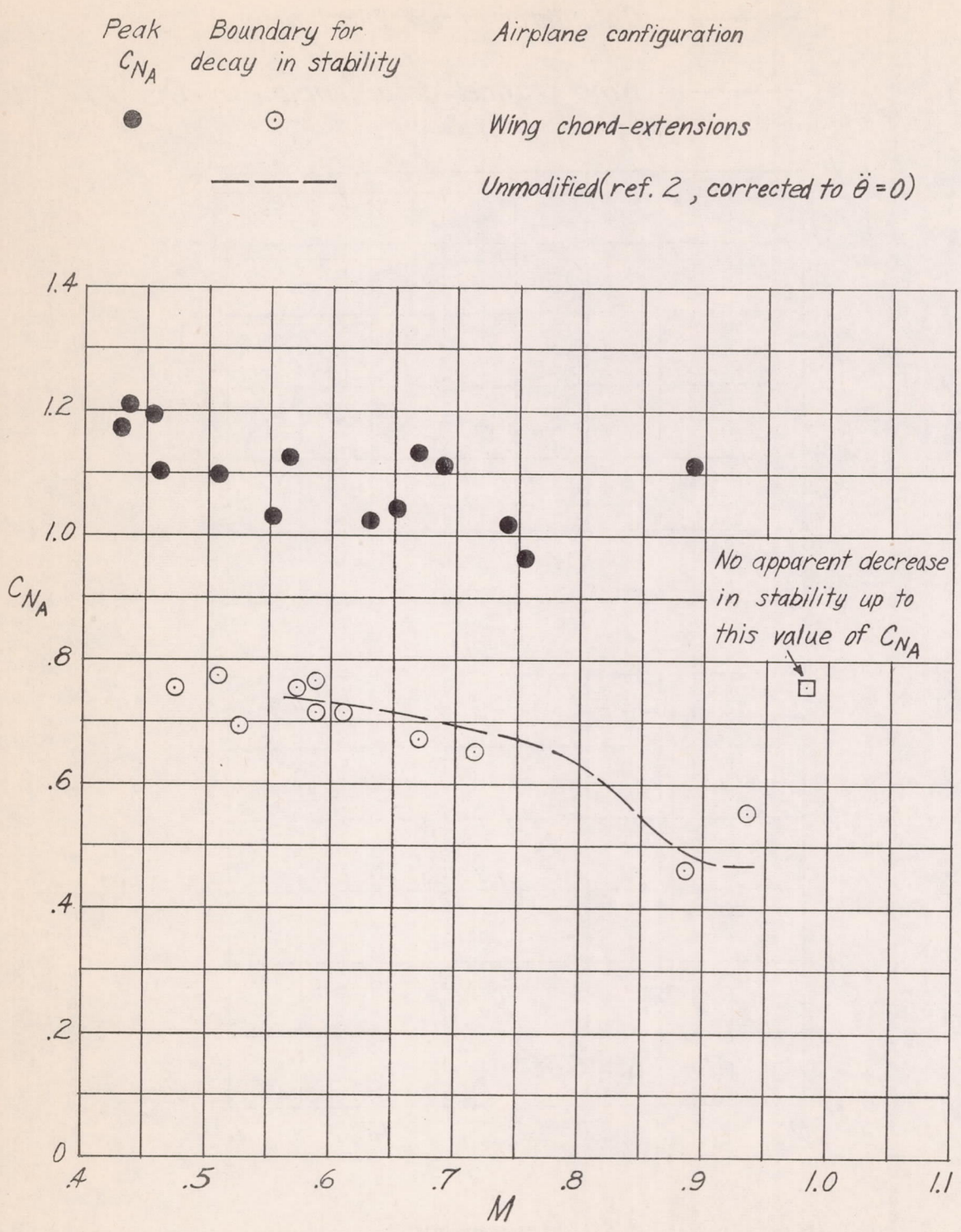

Figure 8.- Normal-force coefficient for decay in longitudinal stability as a function of Mach number for the Douglas D-558-II research airplane.

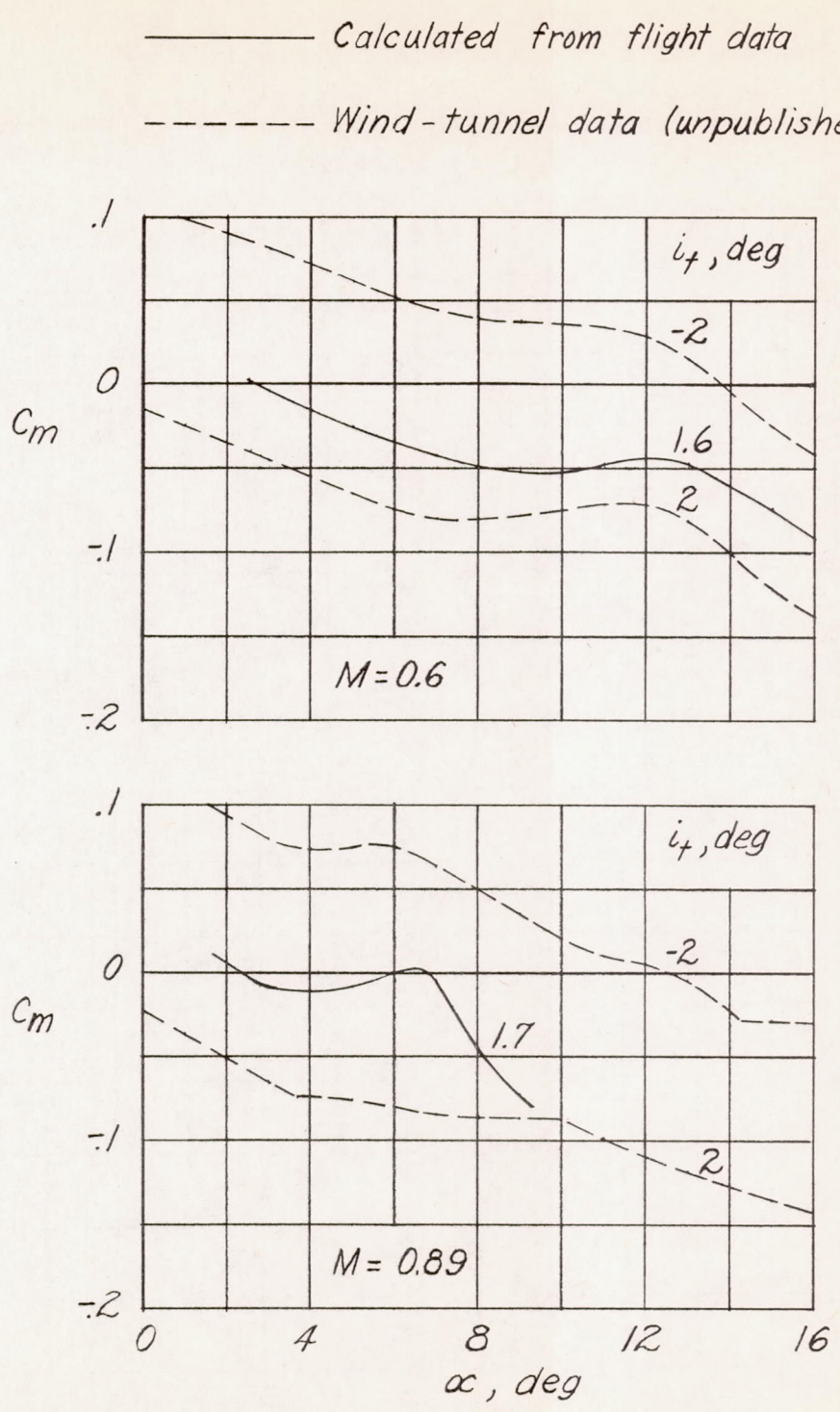

Figure 9.- Comparison of pitching-moment characteristics calculated from flight data with those obtained in the Langley high-speed 7- by 10-foot wind tunnel for the D-558-II airplane equipped with wing leading-edge chord extensions.

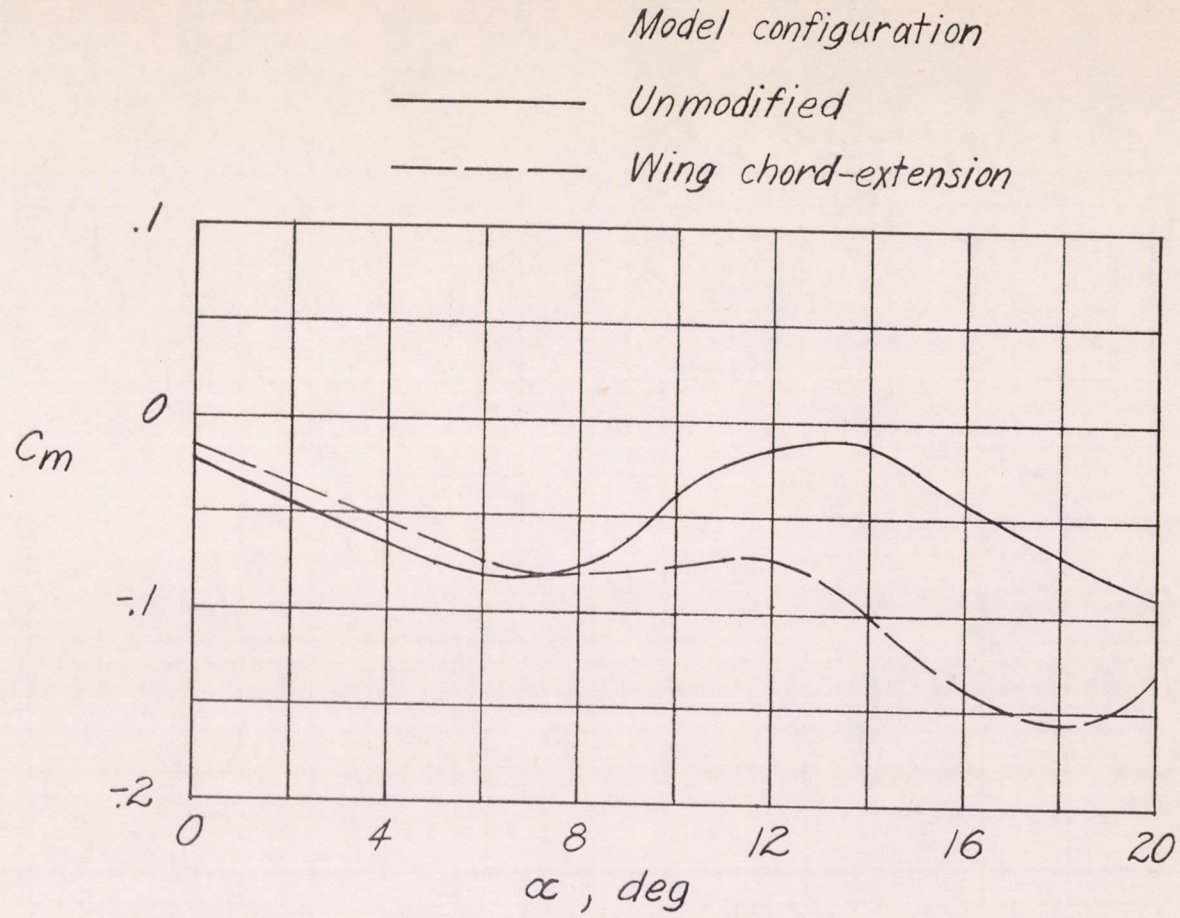

Figure 10.- Variation of pitching-moment coefficient with angle of attack for two model configurations of the D-558-II airplane tested in the Langley high-speed 7- by 10-foot wind tunnel. $M = 0.6$; $i_t = 2^\circ$. (Unpublished data.)

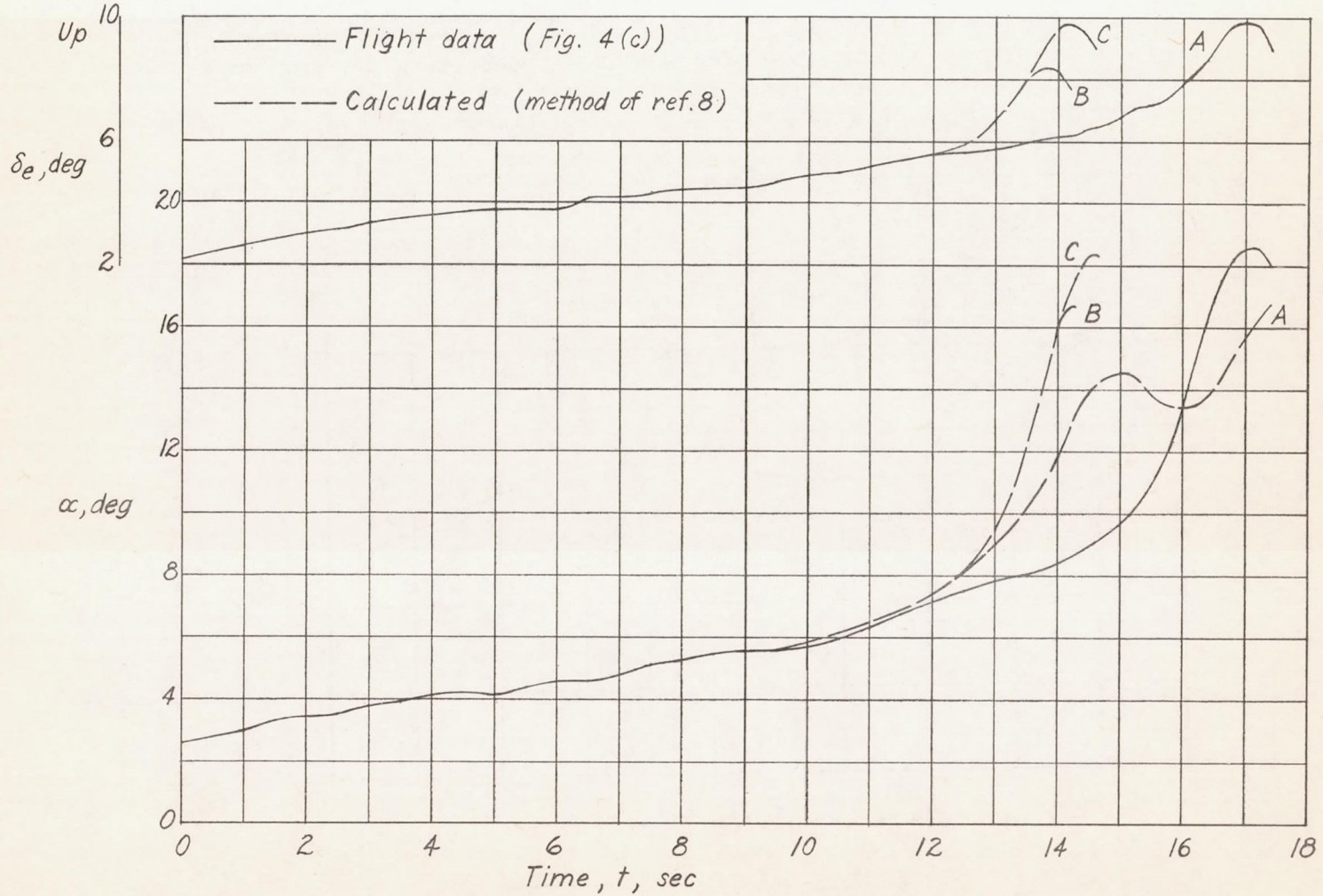

Figure 11.- Time history of flight-measured and calculated accelerated longitudinal maneuvers for the D-558-II research airplane at $M \approx 0.6$. (Calculated data start at 9 seconds.)

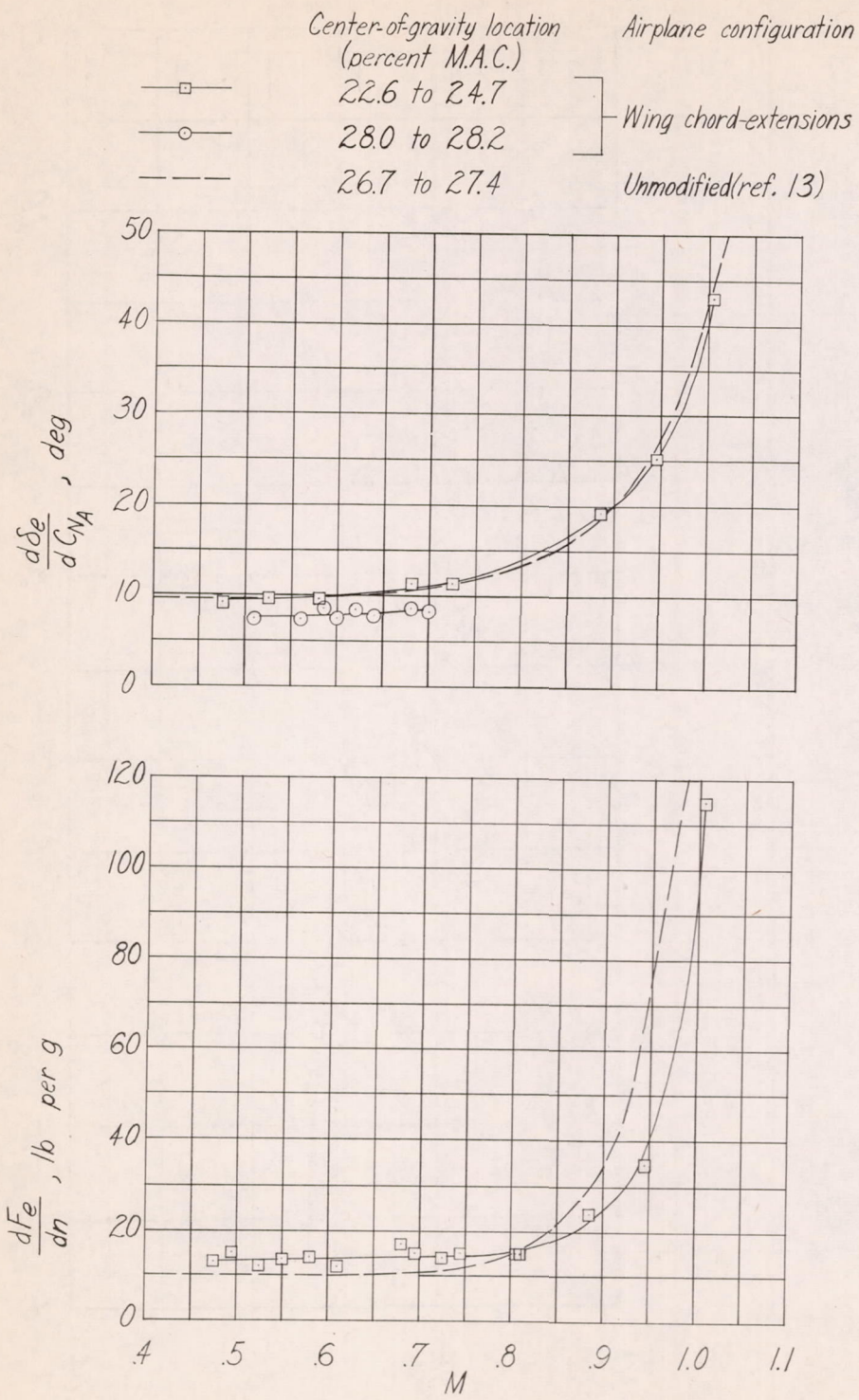

Figure 12.- Variation with Mach number of $d\delta_e/dC_{N_A}$ and dF_e/dn for the Douglas D-558-II research airplane.

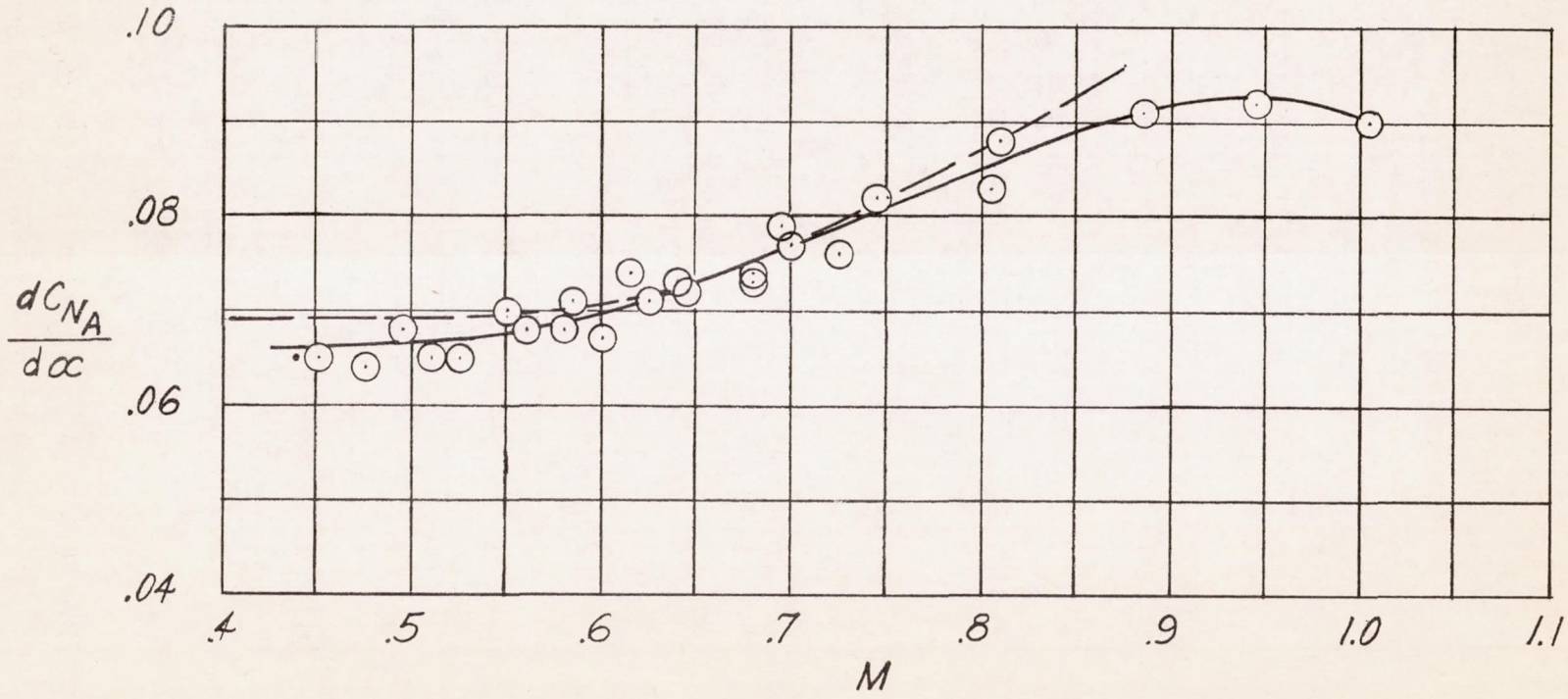

Figure 13.- Variation with Mach number of $dC_{N_A}/d\alpha$ for the Douglas D-558-II research airplane.